Thrombopoietin initiates demethylation-based transcription of *GP6* during megakaryocyte differentiation

Sachiko Kanaji, Taisuke Kanaji, Beatrice Jacquelin, Mei Chang, Diane J. Nugent, Norio Komatsu, Masaaki Moroi, Kenji Izuhara, and Thomas J. Kunicki

Glycoprotein VI (GPVI) is an essential platelet receptor for collagens that is exclusively expressed in the megakaryocytic lineage. Transcription of the human gene *GP6* is driven largely by GATA-binding protein 1 (GATA-1), specificity protein 1 (Sp1), and Friend leukemia integration 1 (Fli-1). In this report, we show that GPVI expression during megakaryocytic differentiation is dependent on cytosine-phosphate-guanosine (CpG) demethylation that can be initiated by thrombopoietin (TPO). Sodium bisulfite genomic sequencing established that a CpG-rich island within the *GP6* promoter region is fully methylated at 10 CpG sites in GPVI-nonexpressive cell lines, such as UT-7/EPO and C8161, but completely unmethylated in GPVI-expressive cell lines, including UT-7/TPO and CHRF288-11. To further confirm the relationship between CpG demethylation and expression of GPVI in primary cells, we treated human cord blood cells with TPO. The *GP6* promoter is highly methylated in cord blood mononuclear cells (progenitors) but not in CD41$^+$-enriched cells obtained after TPO differentiation. Furthermore, when UT-7/EPO-Mpl cells, which stably express human C-myeloproliferative leukemia virus ligand (c-Mpl), were treated with TPO, demethylation of the *GP6* promoter was induced. In every case, demethylation of the *GP6* promoter correlated with an increase in mRNA level. Thus, megakaryocyte-specific expression of the *GP6* gene is regulated, in part, by CpG demethylation, which can be directly initiated by TPO. (Blood. 2005; 105:3888-3892)

Introduction

GP6 is uniquely expressed by cells of the megakaryocyte lineage and encodes platelet glycoprotein VI (GPVI), which figures prominently in collagen-dependent activation and signal transduction.[1] *GP6* transcription requires a number of factors, such as GATA-binding protein 1 (GATA-1), Friend leukemia integration 1 (Fli-1), and specificity protein 1 (Sp1).[2,3] However, the mere presence of these is not sufficient to initiate transcription during megakaryocyte differentiation, since all of these transcription factors are already present in megakaryocyte-erythrocyte progenitors that do not express GPVI. UT-7/TPO is a thrombopoietin (TPO)–dependent human erythro-megakaryocytic human cell line that has an absolute requirement for TPO to induce and maintain proliferation. GPVI is expressed in UT-7/TPO cells cultured in the presence of TPO, but expression declines rapidly (within hours) after TPO starvation. Since the expression of these essential transcription factors is not changed before or after TPO starvation, other mechanisms must be involved in the regulation of megakaryocyte-specific expression of GPVI, and TPO likely initiates these mechanisms.

Methylation of cytosines within the dinucleotide sequence cytosine-phosphate-guanosine (CpG) is probably the most common epigenetic mechanism of transcriptional suppression in vertebrates,[4] and it is widely involved in the establishment and maintenance of cell type–specific gene expression.[5,6] In this study, we show that TPO can initiate the reversal of CpG methylation during human megakaryocyte differentiation leading to the expression of GPVI.

Materials and methods

Sequence analysis

DNA sequences were obtained using an Applied Biosystems ABI Prism Model 377 DNA Sequencer (Perkin-Elmer Applied Biosystems, Foster City, CA) by personnel in the DNA Core Laboratory of the Department of Molecular and Experimental Medicine, The Scripps Research Institute.

Cultured human cell lines

The megakaryocyte cell line CHRF-288-11[7] was a gift from Dr M. A. Lieberman (Cincinnati, OH). The human cell line C8161 was purchased from The American Type Tissue Culture (Manassas, VA). For treatment with 5-aza-2′-deoxycytidine (5-aza-dC; Sigma, St Louis, MO), 6×10^5 cells were cultured in the presence of 10 μM 5-aza-dC in dimethyl sulfoxide (DMSO) for 48 hours.

The erythropoietin (EPO)–dependent cell line UT-7/EPO and the thrombopoietin-dependent cell line UT-7/TPO were established from bone

From The Roon Research Center for Arteriosclerosis and Thrombosis, Division of Experimental Hemostasis and Thrombosis, Department of Molecular and Experimental Medicine, The Scripps Research Institute, La Jolla, CA; the Children's Hospital of Orange County, Orange, CA; the Department of Hematology, University of Yamanashi, Tamaho, Yamanashi, Japan; the Division of Medical Biochemistry, Department of Biomolecular Sciences, Saga Medical School, Saga, Japan; and the Department of Protein Biochemistry, Institute of Life Science, Kurume University, Kurume, Fukuoka, Japan.

Submitted August 13, 2004; accepted December 28, 2004. Prepublished online as *Blood* First Edition Paper, February 8, 2005; DOI 10.1182/blood-2004-08-3109.

Supported by National Heart, Lung, and Blood Institute (NHLBI) grant HL46979 awarded to T.J.K.

Reprints: Thomas J. Kunicki, Department of Molecular and Experimental Medicine, The Scripps Research Institute, 10666 N Torrey Pines Rd, Maildrop MEM150, La Jolla, CA 92037. email: tomk@scripps.edu.

The publication costs of this article were defrayed in part by page charge payment. Therefore, and solely to indicate this fact, this article is hereby marked "advertisement" in accordance with 18 U.S.C. section 1734.

marrow cells obtained from a patient with acute megakaryocytic leukemia.[8,9] UT-7/TPO cells were maintained in liquid culture with Iscoves modified Dulbecco medium (IMDM; Invitrogen, San Diego, CA) containing 10% fetal calf serum (FCS) and 10 ng/mL recombinant human (rh) TPO. UT-7/EPO cells were maintained in the same culture conditions as UT-7/TPO cells, except for the addition of 1 IU/mL rhEPO; both UT-7/EPO and UT-7/TPO were kindly provided by the Kirin Brewery (Gunma, Japan).

Reverse transcriptase–polymerase chain reaction (RT-PCR)

RNA was extracted using ISOGEN (Nippongene, Tokyo, Japan) according to the manufacturer's instructions. Total RNA was reverse transcribed using the GeneAmp RNA PCR kit (Applied Biosystems Japan, Tokyo, Japan). The PCR primers used were as follows: GPVI forward, 5′-CTCAGGACAGGGCTGAGGAA-3′; GPVI reverse, 5′-GGATGAAGAGGACTGCCTGA-3′; glyceraldehyde phosphate dehydrogenase (GAPDH) forward, 5′-GAAGGTGAAGGTCGGAGT-3′; and GAPDH reverse, 5′-CTTCTACCACTACCCTAAAG-3′.

Bisulfite treatment of DNA samples

Genomic DNA (1 μg) was denatured in 50 μL 0.2-M NaOH at 37°C for 20 minutes and then mixed with 30 μL 10-mM hydroquinone (Sigma) and 520 μL 3-M sodium bisulfite (pH 5.0; Sigma). Reactants were incubated at 55°C for 16 hours. Bisulfite-modified DNA was purified using the Wizard purification resin and a Vacuum Manifold (Promega, Madison, WI) and eluted into 50 μL water. After addition of 5.5 μL 3-M NaOH (final 0.3 M), samples were let to stand at 37°C for 20 minutes, then precipitated in ethanol and dissolved in 20 μL water. A fragment of genomic DNA encompassing the CpG island of *GP6* (−264 to +35) was amplified using the following primer pair: forward, 5′-GTGATATTAGGGAGTTTATGGGAGT-3′; and reverse, 5′-AAAACATAATTCCTCAACCCTATCC-3′.

For methylation-specific PCR, dmsp-R1 (5′-TTTCCTAATTAAAACTCATCAAACCA-3′) or msp-R2 (5′-CGACCTTTCCTAATTAAAACTCATCG-3′) was used in combination with the same forward primer described in the previous paragraph.

In the case of established cell lines, PCR products were directly sequenced; when primary mononuclear or CD41-enriched cells, or UT-7/EPO Mpl cells, were studied, the PCR products were gel purified using the QIAquick Gel Extraction kit (Qiagen, Hilden, Germany) and cloned into the pGEM-T easy vector (Promega).

Serum-free liquid culture system for in vitro analysis of megakaryocytopoiesis

Culture was carried out as previously described, with modifications.[10] Briefly, venous cord blood from the umbilical vessels of healthy, full-term infants was collected immediately after delivery and mixed with one quarter volume of 6% hydroxyethyl starch. Erythrocytes were allowed to settle at room temperature for 30 to 45 minutes. Mononuclear cells (MNCs) in the supernatant were then isolated using a Ficoll-Hypaque density gradient, washed, and resuspended for culture, as previously described.[11] The culture system consisted of 1×10^6 MNCs/mL in Iscoves modified Dulbecco medium (Irvine Scientific, Irvine, CA), supplemented with 1% bovine serum albumin (BSA); 75 μM α-thioglycerol; 40 μg/mL each of linoleic acid, lecithin, and cholesterol; 1% Nutridoma Hu (Roche Boehringer Mannheim, Indianapolis, IN); and 30 ng/mL recombinant human thrombopoietin (rhTPO, 288-TPN-005; R&D Systems, Minneapolis, MN). The total number of suspension cells in culture was determined using a CELL-DYN 1600 multiparameter hematology analyzer (Abbott Laboratories, Abbott Park, IL). The day-8 cells were used for the CD41$^+$ cell purification.

Isolation of CD41$^+$ cells

CD41$^+$ cells were isolated using Dynabeads Pan Mouse immunoglobulin G (IgG; Dynal Biotech, Lake Success, NY) and murine anti-CD41 monoclonal antibody (mAb, clone 5B12; DAKO, Carpinteria, CA), according to the manufacturer's instruction (Dynal Biotech). Briefly, Dynabeads Pan Mouse IgG and murine anti-CD41 mAb (0.5-1 μg anti-CD41 mAb/10^7 beads) were incubated at 4°C for 30 minutes and washed. Cultured cells (4×10^7) were then incubated for 30 minutes at 4°C with the anti-CD41–coated beads, and those cells adherent to the beads were separated magnetically.

Isolation of DNA from mononuclear cells and enriched CD41$^+$ cells

DNA from cord blood MNCs or CD41$^+$-enriched cells was purified using the Puregene DNA isolation kit (Gentra Systems, Minneapolis, MN), according to the manufacturer's instruction.

Measurement of surface expression of GPVI

Surface expression of GPVI was measured by flow cytometry using mouse anti-GPVI monoclonal antibody (204-11).[12] Cells were incubated for 20 minutes at 4°C with the appropriately diluted antibody. After a first washing, the cells were incubated with a fluorescein-labeled second antibody for 20 minutes at 4°C. After a second washing, bound antibody was detected using a Facscalibur flow cytometer (Becton Dickinson, San Jose, CA), and data were reported as the geometric mean fluorescence intensity (GMFI).

Results and discussion

As shown in Figure 1A, the proximal 5′-regulatory region of *GP6* contains 10 CpG sites within the segment from −238 to −90, which overlaps the core promoter. We used bisulfite sequencing to analyze the methylation status of these CpG sites in the *GP6* promoter of DNA isolated from various established cell lines. Primers were designed that are complementary to sequences

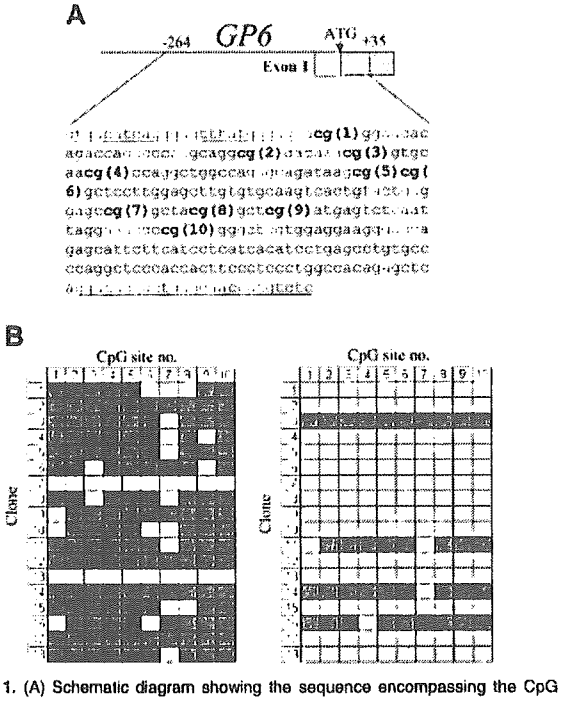

Figure 1. (A) Schematic diagram showing the sequence encompassing the CpG islands within the proximal 5′-regulatory region of human *GP6*. The CpG sites are indicated in bold and numbered consecutively in the 5′ to 3′ direction. The sequences of the flanking primer pairs used to amplify each CpG-rich segment are underlined. (B) Methylation status of the *GP6* CpG island in human cord blood mononuclear cells (left) or enriched CD41$^+$ cells (right). In each grid, each CpG site is represented by a column and indicated at the top, while individual cloned DNA sequences are represented by rows and numbered to the left. ■ indicates methylated CpG sites; □, unmethylated sites. Numbers at the top correspond to the same CpG sites shown in panel A. In MNC precursors, 16 (89%) of 18 clones showed methylation at 7 or more of the 10 sites; and in the CD41$^+$-enriched population, only 4 (22%) of 18 clones showed methylation at 8 or more sites.

flanking this region and lacking CpG dinucleotides, in order to permit amplification of all genomic sequences, regardless of the status of methylation.

In GPVI-expressive cell lines, such as CHRF-288-11 and UT-7/TPO, these CpG sites are unmethylated, while the corresponding tract in genomic DNA of the GPVI-nonexpressive cell lines C8161 and UT-7/EPO is fully methylated (data not shown). These results establish that the expression of GPVI correlates with the CpG methylation status of the proximal 5′-regulatory region.

To obtain a more accurate evaluation of a role for CpG methylation in expression of these genes during megakaryocytic differentiation, we turned to the study of primary human megakaryocytes. We isolated mononuclear cells (MNCs) from human cord blood, cultured these in the presence of rhTPO for 8 days, and then selected the CD41$^+$ cells. The methylation status of the *GP6* promoter region of CpG islands was then compared between rhTPO-stimulated CD41$^+$-enriched (megakaryocyte enriched) cells and the MNCs from which they were derived.

In the initial MNC population, megakaryocytes and progenitors may represent no more than 5% to 10% of the total cell population. The allelic methylation status is shown in Figure 1B. In MNCs, 16 of 18 clones showed substantial methylation (at least 7 of the 10 possible CpG sites), whereas the majority of DNA clones obtained from the CD41$^+$-enriched population now contained unmethylated CpG sites (14 of 18). These results suggest that megakaryocyte differentiation is characterized by a decrease in CpG methylation of the *GP6* proximal 5′-regulatory region. Because of the difficulty in obtaining adequate numbers of primary megakaryocytes in sufficient purity, the CD41$^+$-enriched population we used contains a significant proportion of CD41$^-$ or CD41-low cells. Thus, it is highly likely that contamination by these cells contributes to the proportion of unmethylated CpG detected in the CD41$^+$-enriched preparations.

To directly show that CpG methylation plays an important role in the regulation of GPVI expression during megakaryocyte differentiation, we elected to differentiate a homogeneous non-megakaryocytic cell line with TPO. UT-7/EPO is an erythropoietin (EPO)–dependent human leukemic cell line that does not express endogenous c-Mpl. The related cell line UT-7/EPO-Mpl stably expresses exogenously introduced c-mpl cDNA and can be differentiated by TPO.[13] We treated UT-7/EPO-Mpl with TPO and examined the expression of *GP6* by RT-PCR (Figure 2A, upper panel). UT-7/EPO-Mpl cells do not express GPVI when they are grown in the presence of EPO. Expression of GPVI was detected

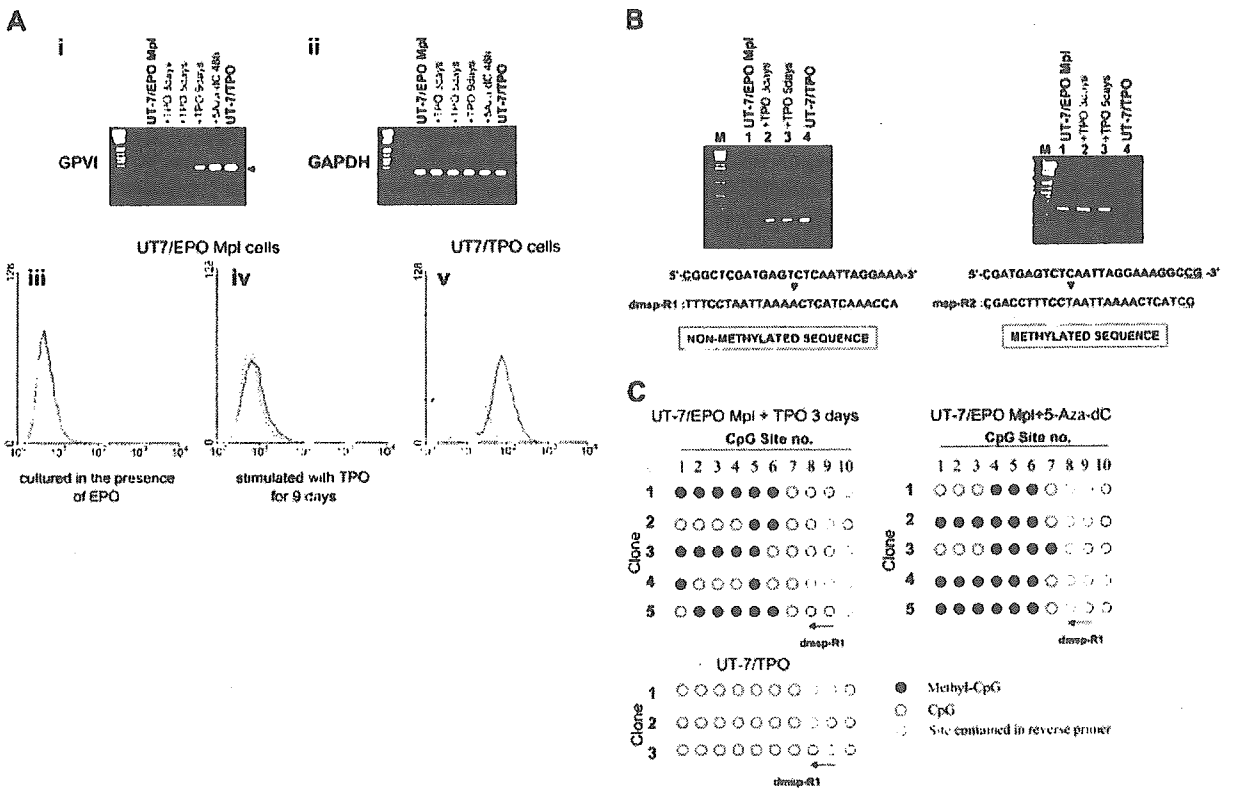

Figure 2. (A, i-ii) TPO induced expression of GPVI on UT-7/EPO Mpl cells. Total RNA was extracted from cells treated with 10 ng/mL TPO for 3, 5, or 9 days or with 10 μM 5-aza-dC for 48 hours. GPVI (i) and GAPDH (ii) mRNA were then amplified by RT-PCR. By this method, GPVI mRNA was detected in cells treated with TPO for 5 or 9 days or in cells treated with 5-aza-dC. (iii-v) Surface expression of GPVI by UT-7/EPO Mpl cells treated with TPO, as determined by flow cytometry. — represents binding of the murine monoclonal antihuman GPVI antibody 204-11; --- corresponds to staining with fluorescein isothiocyanate–labeled secondary antibody alone. (iii) No binding was observed when UT-7/EPO Mpl are cultured in the presence of EPO. (iv) Weak, but reproducible, binding was observed following culture of UT-7/EPO Mpl in the presence of TPO for 9 days. (v) Intense binding is observed when UT-7/TPO are cultured in the presence of TPO. These results are representatives of identical findings made in 3 independent experiments. (B) Methylation-specific PCR of the *GP6* promoter CpG island. Reverse primers were designed to distinguish the unmethylated (left) or methylated (right) DNA. The methylation-negative primer dmsp-R1 includes the eighth and ninth CpG sites converted to TG; in the methylation-positive primer msp-R2, the ninth CpG site is conserved as CG. The *GP6* product (170 bp) is obtained using dmsp-R1 only when the cells are treated with TPO. (C) Methylation status of *GP6* CpG sites in the product amplified with dmsp-R1 and shown in panel B. DNA was isolated from UT-7/EPO Mpl cells stimulated with TPO for 3 days or 5-aza-dC for 48 hours and treated with sodium bisulfite. PCR was performed with the same forward primer used in Figure 1B and dmsp-R1 used as the reverse primer. Amplified DNA was cloned into pGEM-T easy vector, and the methylation status was determined by DNA sequencing. ● indicates methylated CpG sites; ○, unmethylated sites; and), sites contained within the reverse primers. Numbers at the top correspond to the same CpG sites shown in Figure 1A.

when cells were treated with 5-aza-dC for 48 hours, which suggests that inactivation of *GP6* in this cell line is caused by methylation. De novo expression of GPVI was also detected when the cells were cultured in the presence of TPO but not EPO for 5 days. We also analyzed surface expression of GPVI by flow cytometry and detected very low but reproducible expression of GPVI after TPO differentiation (Figure 2A, lower panel).

To confirm that TPO-induced expression of GPVI occurs via demethylation of the *GP6* promoter, we next assessed the methylation status of the *GP6* promoter region (Figure 2B). In this case, sodium bisulfite–treated genomic DNA was amplified with 2 kinds of reverse primers, which anneal specifically to either unmethylated (dmsp-R1) or methylated (msp-R2) sequences. We used these primers in order to more efficiently detect the small population of demethylated alleles that would otherwise have been obtainable by sequencing a large number of alleles amplified with the primers used in the experiments described in Figure 1B. By this approach, product is obtained with the dmsp-R1 primer (specific for the unmethylated sequence) only when UT-7/EPO-Mpl cells are cultured in the presence of TPO (Figure 2Bi). Nothing is detected when they are cultured in the presence of EPO. In contrast, a detectable product is obtained from UT-7/EPO-Mpl cells with the msp-R2 primer (specific for the methylated sequence) when these are cultured either in the presence of rhEPO or rhTPO (Figure 2Bii). At the same time, no product is obtained from UT-7/TPO cells.

Thus, we detected PCR product amplified with dmsp-R1 when UT-7/EPO Mpl cells were maintained in the presence of TPO. This product was cloned into the pGEM-T easy vector, and individual DNA clones were characterized by direct sequencing. As shown in Figure 2C, 43% of CpG sites in the 5′-regulatory region of *GP6* were unmethylated in the alleles amplified with dmsp-R1. These results confirmed that TPO induced partial demethylation and expression of the *GP6* gene in UT-7/EPO-Mpl cells. Although GPVI mRNA is maximally up-regulated when these cells are differentiated with TPO for 9 days, the methylation status is not significantly changed between 3 and 9 days of TPO differentiation. Additional factors, not expressed by this cell line, may be required for complete demethylation and full expression of GPVI.

The demethylation of the *GP6* promoter and surface expression of GPVI initially observed in primary megakaryocytes (Figure 1B) was mimicked by these established UT-7 cell lines, but the extent of methylation/demethylation was not as dramatic as in the primary cells. Since UT-7/EPO was established from UT-7 by prolonged selection in the presence of EPO, it may well be that this subline is so extensively differentiated into an erythroid lineage that it is not possible to completely dedifferentiate and redifferentiate the cell line into a full megakaryocyte lineage.

To distinguish whether demethylation of the *GP6* promoter is directly linked to signal induction by TPO or merely a nonspecific result of the differentiation of these cells, we assayed the demethylation status of UT-7/TPO grown in the presence of granulocyte-macrophage colony-stimulating factor (GM-CSF) for 2 days. As shown in Figure 3A, the surface expression of GPVI decreased following culture in the presence of GM-CSF. Using methylation-specific PCR, we also obtained a product with the msp-R2 primer only when UT-7/TPO cells were grown in the presence of GM-CSF (Figure 3B). This product was cloned into the pGEM-T easy vector for sequencing, and 17% of CpG sites were methylated in the alleles amplified with msp-R2 (data not shown). These results support the contention that demethylation and expression of *GP6* are not an indirect effect of the differentiation state of the cells but a direct consequence of TPO signaling.

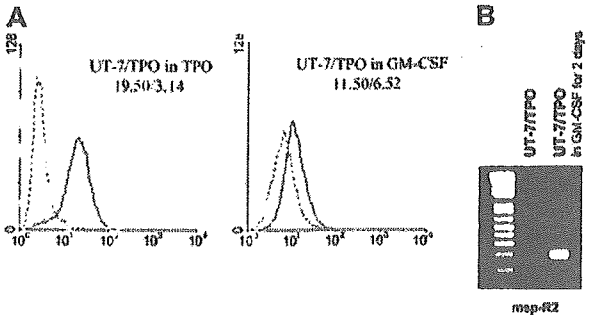

Figure 3. Lack of effect of nonspecific differentiation upon demethylation. (A) Surface expression of GPVI by UT-7/TPO cells cultured in the presence of GM-CSF. UT-7/TPO cells were cultured in the presence of 1 ng/mL GM-CSF for 2 days, and surface expression of GPVI was analyzed by flow cytometry using antibody 204-11 (—). ··· corresponds to staining with fluorescein isothiocyanate–labeled secondary antibody alone. The respective GMFI for each tracing is indicated in the respective panel, and these results are representative of 3 independent experiments. (B) Methylation-specific PCR of the *GP6* promoter in UT-7/TPO cells cultured in the presence of GM-CSF. The reverse primer msp-R2 was used to specifically amplify methylated alleles. A product was obtained when UT-7/TPO were cultured in the presence of GM-CSF (right lane) but not when they were cultured in the presence of TPO (center lane).

Certain genes with restricted expression to hematopoietic cells, such as the genes for myeloperoxidase,[14] globin,[15] c-fms,[16] and the granulocyte colony-stimulating factor (G-CSF) receptor,[17] are regulated by methylation in a lineage- and differentiation-dependent manner. Megakaryocyte-specific gene induction, however, has not yet been associated with changes in promoter CpG methylation. As the CpG island is located in the core promoter of *GP6* and some of CpG sites reside close to the binding sites for essential transcription factors, CpG methylation may directly interfere with the binding of transcriptional activators, or conversely, enhance the binding of transcriptional repressors.

Although TPO is the principal regulator of megakaryopoiesis and thrombocytopoiesis, it is not known whether it is directly involved in the mechanisms that regulate CpG methylation. Our results establish, for the first time, a role for TPO in dynamic changes in CpG methylation status that are involved in the epigenetic regulation of megakaryocyte-specific gene expression.

Acknowledgments

We thank Dr Jerry Ware (The Scripps Research Institute, La Jolla, CA) for his advice and support during these studies and Diana Rozenshteyn for her technical assistance. This is manuscript number 14045-MEM from The Scripps Research Institute.

References

1. Clemetson KJ, Clemetson JM. Platelet collagen receptors. Thromb Haemost. 2001;86:189-197.
2. Furihata K, Kunicki TJ. Characterization of human glycoprotein VI gene 5′ regulatory and promoter regions. Arterioscler Thromb Vasc Biol. 2002;22:1733-1739.
3. Holmes ML, Bartle N, Eisbacher M, Chong BH. Cloning and analysis of the thrombopoietin-induced megakaryocyte-specific glycoprotein VI promoter and its regulation by GATA-1, Fli-1, and Sp1. J Biol Chem. 2002;277:48333-48341.
4. Lu Q, Ray D, Gutsch D, Richardson B. Effect of DNA methylation and chromatin structure on ITGAL expression. Blood. 2002;99:4503-4508.
5. Futscher BW, Oshiro MM, Wozniak RJ, et al. Role for DNA methylation in the control of cell type specific maspin expression. Nat Genet. 2002;31:175-179.

6. Uhl J, Klan N, Rose M, et al. The 5-lipoxygenase promoter is regulated by DNA methylation. J Biol Chem. 2002;277:4374-4379.
7. Fugman DA, Witte DP, Jones CLA, Aronow BJ, Lieberman MA. In vitro establishment and characterization of a human megakaryoblastic cell line. Blood. 1990;75:1252-1261.
8. Komatsu N, Kunitama M, Yamada M, et al. Establishment and characterization of the thrombopoietin-dependent megakaryocytic cell line, UT-7/TPO. Blood. 1996;87:4552-4560.
9. Komatsu N, Yamamoto M, Fujita H, et al. Establishment and characterization of an erythropoietin-dependent subline, UT-7/Epo, derived from human leukemia cell line, UT-7. Blood. 1993;82:456-464.
10. Chang M, Nakagawa PA, Williams SA, et al. Immune thrombocytopenic purpura (ITP) plasma and purified ITP monoclonal autoantibodies inhibit megakaryocytopoiesis in vitro. Blood. 2003;102:887-895.
11. Chang M, Suen Y, Lee SM, et al. Transforming growth factor-beta 1, macrophage inflammatory protein-1 alpha, and interleukin-8 gene expression is lower in stimulated human neonatal compared with adult mononuclear cells. Blood. 1994;84:118-124.
12. Moroi M, Mizuguchi J, Kawashima S, et al. A new monoclonal antibody, mAb 204-11, that influences the binding of platelet GPVI to fibrous collagen. Thromb Haemost. 2003;89:996-1003.
13. Takatoku M, Kametaka M, Shimizu R, Miura Y, Komatsu N. Identification of functional domains of the human thrombopoietin receptor required for growth and differentiation of megakaryocytic cells. J Biol Chem. 1997;272:7259-7263.
14. Lubbert M, Miller CW, Koeffler HP. Changes of DNA methylation and chromatin structure in the human myeloperoxidase gene during myeloid differentiation. Blood. 1991;78:345-356.
15. Enver T, Zhang JW, Anagnou NP, Stamatoyannopoulos G, Papayannopoulou T. Developmental programs of human erythroleukemia cells: globin gene expression and methylation. Mol Cell Biol. 1988;8:4917-4926.
16. Felgner J, Kreipe H, Heidorn K, et al. Lineage-specific methylation of the c-fms gene in blood cells and macrophages. Leukemia. 1992;6:420-425.
17. Felgner J, Heidorn K, Korbacher D, Frahm SO, Parwaresch R. Cell lineage specificity in G-CSF receptor gene methylation. Leukemia. 1999;13:530-534.

THE JOURNAL OF BIOLOGICAL CHEMISTRY

Vol. 280, No. 26, Issue of July 1, pp. 24915–24922, 2005
Printed in U.S.A.

Characterization of the Interaction between Interleukin-13 and Interleukin-13 Receptors*

Received for publication, March 8, 2005, and in revised form, April 21, 2005
Published, JBC Papers in Press, May 3, 2005, DOI 10.1074/jbc.M502571200

Kazuhiko Arima‡, Kazuo Sato§¶, Go Tanaka‡, Sachiko Kanaji‡, Tohru Terada§‖, Eijiro Honjo, Ryota Kuroki**, Yo Matsuo§¶, and Kenji Izuhara‡ ‡‡§§**

*From the ‡Division of Medical Biochemistry, Department of Biomolecular Sciences, and the ‡‡Division of Medical Research, Center for Comprehensive Community Medicine, Saga Medical School, Saga 849-8501, the §Computational Proteomics Team, Protein Research Group, RIKEN Genomic Sciences Center, Yokohama 230-0045, the ¶Graduate School of Integrated Sciences, Yokohama City University, Yokohama 230-0045, the ‖Graduate School of Agricultural and Life Sciences, Faculty of Agriculture, The University of Tokyo, Tokyo 113-8657, and the **Structural Biology Group, Neutron Science Research Center, Japan Atomic Energy Research Institute, Ibaraki 319-1195, Japan*

Interleukin-13 (IL-13) possesses two types of receptor: the heterodimer, composed of the IL-13Rα1 chain (IL-13Rα1) and the IL-4Rα chain (IL-4Rα), transducing the IL-13 signals; and the IL-13Rα2 chain (IL-13Rα2), acting as a nonsignaling "decoy" receptor. Extracellular portions of both IL-13Rα1 and IL-13Rα2 are composed of three fibronectin type III domains, D1, D2, and D3, of which the last two comprise the cytokine receptor homology modules (CRHs), a common structure of the class I cytokine receptor superfamily. Thus far, there has been no information about the critical amino acids of the CRHs or the role of the D1 domains of IL-13Rα1 and IL-13Rα2 in binding to IL-13. In this study, we first built the homology modeling of the IL-13·hIL-13 receptor complexes and then predicted the amino acids involved in binding to IL-13. By incorporating mutations into these amino acids, we identified Tyr-207, Asp-271, Tyr-315, and Asp-318 in the CRH of human IL-13Rα2, and Leu-319 and Tyr-321 in the CRH of human IL-13Rα1, as critical residues for binding to IL-13. Tyr-315 in IL-13Rα2 and Leu-319 in IL-13Rα1 are positionally conserved hydrophobic amino acid residues. Furthermore, by using D1 domain-deleted mutants, we found that the D1 domain is needed for the expression of IL-13Rα2, but not IL-13Rα1, and that the D1 domain of IL-13Rα1 is important for binding to IL-13, but not to IL-4. These results provide the basis for a precise understanding of the interaction between IL-13 and its receptors.

Interleukin (IL)[1]-13 is a pleiotropic Th-2-type cytokine produced by $CD4^+$ T cells, natural killer T cells, mast cells, basophils, and eosinophils (1). It is known that IL-13 plays a pivotal role in host defense against parasite infection and in the pathogenesis of allergic diseases (1–3). IL-13 exerts its actions by binding to the IL-13 receptor (IL-13R) on the cell surface, the heterodimer comprised of the IL-13Rα1 chain (IL-13Rα1) and the IL-4Rα chain (IL-4Rα). IL-13 binds to IL-13Rα1 first with low affinity (K_d = 2–10 nM) and then recruits IL-4Rα to the complex, generating a high affinity receptor (K_d = 0.03–0.4 nM) (4–6). Heterodimerization of IL-13R causes activation of Janus kinases, TYK2 and JAK1, constitutively associated with IL-13Rα1 and IL-4Rα, respectively, followed by activation of the signal transducer and activator of transcription 6 (STAT6) (1). STAT6 is a transcription factor critical for IL-13 signals, causing expression of various IL-13-inducible genes together with other transcriptional factors (1, 7). There is another IL-13-binding unit, the IL-13Rα2 chain (IL-13Rα2), which binds to IL-13 with high affinity (0.25–1.2 nM) (8, 9). No other receptor molecule is known to be involved in the IL-13·IL-13Rα2 complex. IL-13Rα2 is thought to act as a nonsignaling "decoy" receptor because its cytoplasmic tail is short and does not contain any obvious signaling motif (10, 11). Consistent with this notion, IL-13Rα2-disrupted mice showed enhanced IL-13 responses (12, 13). Thus, the two IL-13-binding molecules, IL-13Rα1 and IL-13Rα2, have different affinities with IL-13 and opposite roles in signal transduction, which would cooperate with each other in tuning the IL-13 signals in the body.

The extracellular domains of all members of the class I cytokine receptor superfamily, including IL-13Rα1 and IL-13Rα2, contain the cytokine receptor homology module (CRH), composed of two fibronectin type III (FnIII) domains (14). Each domain consists of ~100 amino acid residues, generating a β-sandwich structure where seven β-strands are arranged in the Greek key topology analogous to an immunoglobulin-constant domain. Four positionally conserved cysteine residues in the first FnIII domain form two disulfide bonds, and a WSXWS sequence locates in the F′-G′ loop in the second FnIII domain, both of which are critical for the receptors to position correctly and bind to ligands (14). Crystal structural analyses of the ligand-receptor complexes of growth hormone (GH), erythropoietin, IL-4, IL-6, IL-12, and the granulocyte colony-stimulating factor (G-CSF) have demonstrated that several loops of the CRHs of these receptors provide binding interfaces composed of hydrophobic and polar amino acids (15–20).

The extracellular domains of a subgroup of the class I cytokine receptor superfamily (gp130, G-CSFR, the granulocyte/macrophage colony-stimulating factor receptor α chain, the leukemia inhibitory factor receptor (LIFR), IL-3Rα, and IL-

* This work was supported in part by a research grant for immunology, allergy, and organ transplant from the Ministry of Health, Welfare, and Labor of Japan, a grant-in-aid for scientific research from the Japan Society for the Promotion of Science, and a grant from Mitsubishi Pharma Research Foundation. The costs of publication of this article were defrayed in part by the payment of page charges. This article must therefore be hereby marked "*advertisement*" in accordance with 18 U.S.C. Section 1734 solely to indicate this fact.

§§ To whom correspondence should be addressed: Division of Medical Biochemistry, Dept. of Biomolecular Sciences, Saga Medical School, Saga 849-8501, Japan. E-mail: kizuhara@med.saga-u.ac.jp.

[1] The abbreviations used are: IL, interleukin; Ab, antibody; CRH, cytokine receptor homology; FnIII, fibronectin type III; γc, common γ chain; G-CSF, granulocyte colony-stimulating factor; GH, growth hormone; h, human; HA, hemagglutinin; HEK, human embryonic kidney; IL-4Rα, IL-4Rα chain; IL-13R, IL-13 receptor; IL-13Rα1 and IL-13Rα2, IL-13Rα1 and α2 chains; LIF, leukemia inhibitory factor; PRL, prolactin; STAT6, signal transducer and activator of transcription 6; R, receptor.

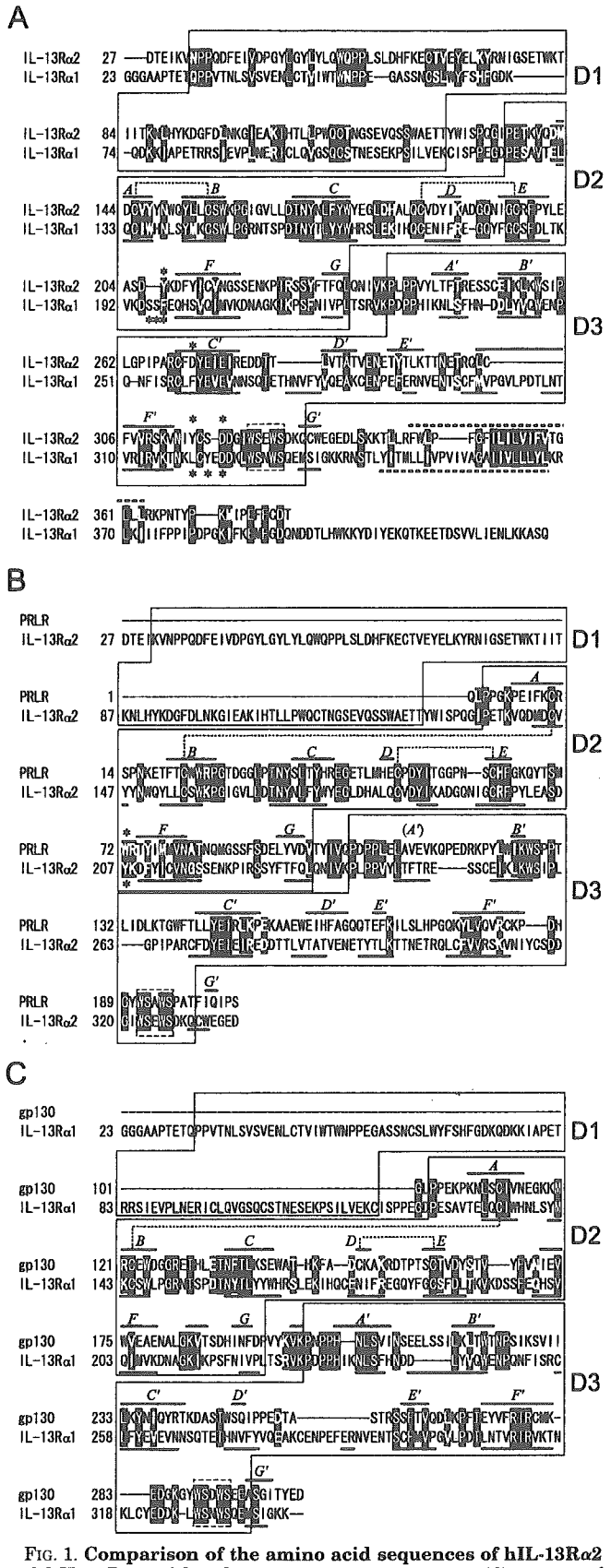

FIG. 1. **Comparison of the amino acid sequences of hIL-13Rα2 and hIL-13Rα1 with other receptor components.** Alignments of the amino acid sequences between hIL-13Rα2 and hIL-13Rα1 (*A*), extracellular portions of human PRLR and hIL-13Rα2 (*B*), and extracellular portions of gp130 lacking the D1 domain and hIL-13Rα1 (*C*) are depicted. The *black* and *gray boxed* amino acids represent identical and homologous amino acids, respectively. The conserved disulfide bonds (*gray solid dashed lines*) and the WSXWS sequences (*dashed line* boxes), characteristics of the class I cytokine receptor superfamily, are indicated. The *thick dashed lines* represent the predicted transmembrane portions. The *asterisks* indicate Ser-195, Ser-196, Phe-197, Leu-319, Tyr-321, and Asp-323 of hIL-13Rα1; Tyr-207, Asp-271, Tyr-315, Asp-318 of hIL-13Rα2; and Trp-72 of PRLR.

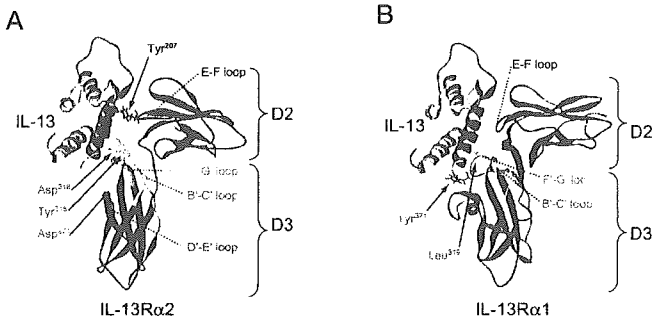

FIG. 2. **Homology modelings of the IL-13·hIL-13Rα2 and IL-13·hIL-13Rα1 complexes.** *A*, homology modeling of the D2 and D3 domains of the IL-13·hIL-13Rα2 complex was built based on the x-ray structure of the GH·PRLR 1:1 complex (PDB code 1BP3) as a template. The E-F, B′-C′, D′-E′, and F′-G′ loops of hIL-13Rα2 are colored in *red*, *yellow*, *orange*, and *green*, respectively. Residues that were replaced by Ala in 4A-mut (Tyr-207, Asp-271, Tyr-315, and Asp-318) are depicted. The *pink* portion represents α-helix D of IL-13. *B*, homology modeling of the IL-13·hIL-13Rα1 complex was built based on the x-ray structure of the viral IL-6·gp130 complex (PDB code 1I1R) and the IL-13·hIL-13Rα2 modeling as templates. The E-F, B′-C′, and F′-G′ loops of hIL-13Rα1 are colored in *red*, *yellow*, and *green*, respectively. Leu-319 and Tyr-321 of hIL-13Rα1 are depicted. The *pink* portion represents α-helix D of IL-13.

5Rα) possess an extra FnIII domain in addition to the CRH. Although even in these receptors, it has been thought that ligand binding is driven principally by the CRH structure, several lines of evidence have shown that the extra FnIII domains of these receptors are also important for the ligand binding. Involvement of the extra FnIII domains of gp130, G-CSFR, LIFR, and IL-5Rα in binding to the ligands has been verified by biochemical analyses (21–27). Furthermore, the x-ray structure of the IL-6·IL-6Rα·gp130 complex shows that the extra FnIII domain of gp130 has a bridging function, interacting with the binding epitope on IL-6 in the opposite trimer, generating the hexametric receptor complex (18, 28).

The extracellular domains of human IL-13Rα1 (hIL-13Rα1) and hIL-13Rα2 have ~33% homology and ~21% identity (Fig. 1*A*). Both are composed of three FnIII domains, D1, D2, and D3 (numbering from the N terminus), of which D2 and D3 comprise the CRHs. The most homologous receptor molecules of hIL-13Rα1 and hIL-13Rα2 in their extracellular domains are hIL-5Rα (44% for hIL-13Rα1 and 45% for hIL-13Rα2, respectively). Mutagenesis analyses of IL-13 have been performed extensively, identifying the amino acid residues important for binding to IL-13 receptors (29–31). However, there has been no information about the critical amino acids of the CRHs of IL-13Rα1 and IL-13Rα2 for binding to IL-13, and the role of the D1 domain in IL-13Rα1 and IL-13Rα2 has been unknown.

In this study, we first built the homology modeling of the IL-13·hIL-13 receptor complexes and then identified critical residues in the CRHs of hIL-13Rα1 or hIL-13Rα2 by mutagenesis analyses, based on these models. Furthermore, we analyzed the roles of the D1 domains in IL-13Rα1 and IL-13Rα2 in their expression and binding to IL-13 and IL-4.

MATERIALS AND METHODS

Reagents and Cells—Recombinant human IL-13 was expressed in *Escherichia coli* transformant-harboring pET28a vector (Novagen, Madison, WI) in which the DNA encoding human IL-13 was inserted. The expressed IL-13 was purified by nickel-nitrilotriacetic acid resin (Qiagen) followed by refolding in 0.1 M Tris-HCl, pH 8.5, containing 3 M

A

IL-13Rα2	*Kd* pM	Binding Sites sites/cell
Wild Type	197±43	2100 ~ 6400
4A-mut	no binding	-
E-F loop		
Asp^{206} → Gln	233±41	710 ~ 2300
Tyr^{207} → Ala	881±249*	2400 ~13000
B'-C' loop		
Ala^{267} → Asp	248±55	850 ~16000
Arg^{268} → Met	189±12	1800 ~ 3500
Asp^{271} → Ala	327±133*	5300 ~ 7000
Asp^{271} → Gln	272±89	2700 ~ 6300
D'-E' loop		
Glu^{289} → Ala	235±35	3400 ~ 4900
Glu^{289} → Gln	242±6.8	3600 ~ 4000
Glu^{291} → Ala	220±47	1900 ~ 9300
Glu^{291} → Gln	211±37	2200 ~ 2900
Glu^{289} → Ala/ Glu^{291}→ Ala	352±31*	2400 ~13000
Glu^{289} → Gln/ Glu^{291} → Gln	206±52	1900 ~ 3900
F'-G' loop		
Tyr^{315} → Ala	437±86*	1000 ~ 8600
Ser^{317} → Ala	242±54	2600 ~ 5900
Asp^{318} → Ala	1113±29*	1500 ~36000
Asp^{318} → Gln	620±140*	2400 ~10000
Asp^{319} → Gln	232±33	2400 ~ 2500
B'-C'/F'-G' loops		
Asp^{271} → Ala/ Asp^{318} → Ala	1406±9.9*	10000 ~25000

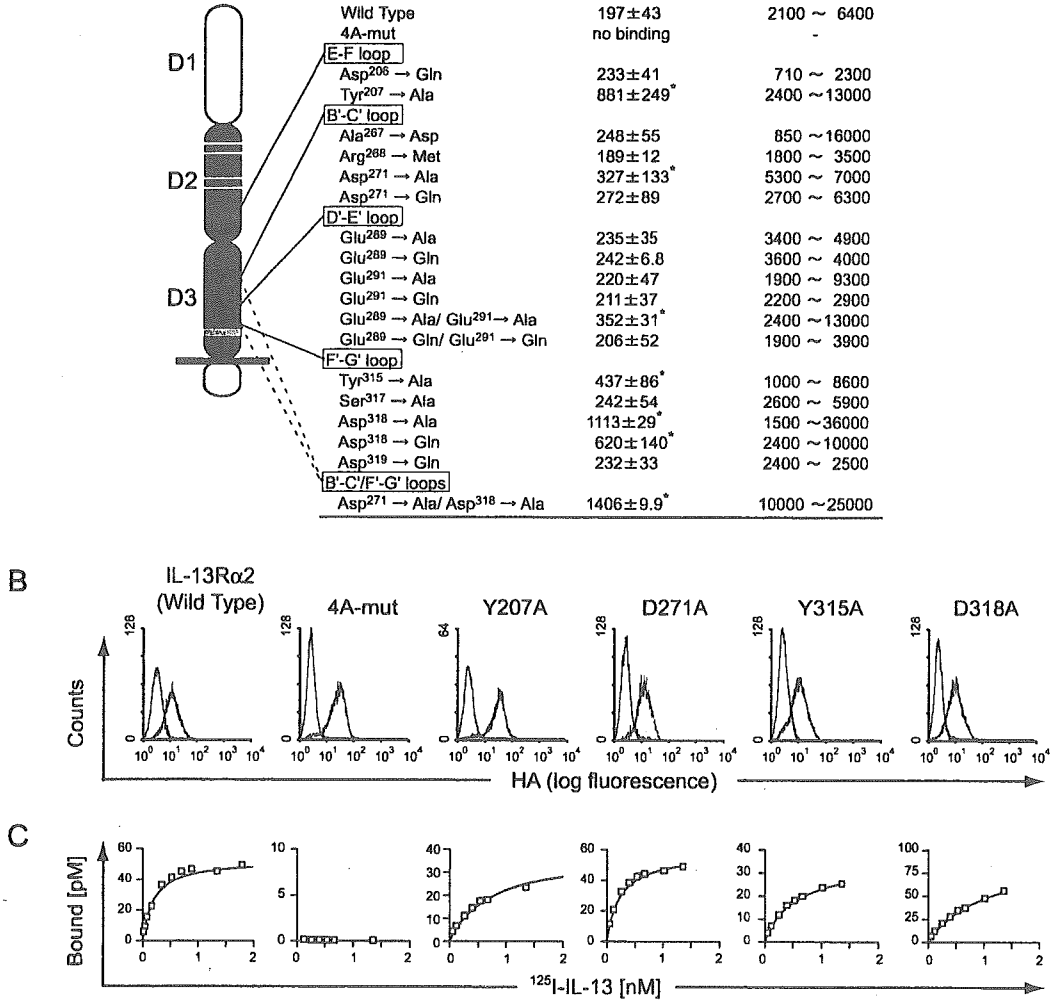

FIG. 3. **Characterization of the mutated types of hIL-13Rα2.** *A*, schematic model of mutated types of hIL-13Rα2 and their K_d values with IL-13 using stable DND-39 transfectants. Experiments were done at least twice for one clone in at least two different clones, and statistical differences with $p < 0.05$ (*) are indicated. The *white bands* in the D2 domain and the *gray band* in the D3 domain represent the conserved cysteine residues and the WSXWS sequence. *B*, expression of hIL-13Rα2 on the surface of DND-39 cells stably transfected with hIL-13Rα2 (wild type, 4A-mut, Y207A, D271A, Y315A, D318A) by flow cytometry. The *shaded* and *open areas* represent the counts with or without the first Ab, respectively. *C*, binding assay of DND-39 cells stably transfected with hIL-13Rα2 (wild type, 4A-mut, Y207A, D271A, Y315A, D318A).

urea, 30% glycerol, 5 mM cysteine, and 5 mM cystamine for 4 days at 4 °C. IL-13 was further purified by SP-Sepharose Fast Flow column chromatography (Amersham Biosciences) and then TSKgel SP5-PW column chromatography (Tosoh, Tokyo, Japan). Detailed expression results of human IL-13 will be published elsewhere.[2] Recombinant human IL-4 was purchased from PeproTech (Rocky Hill, NJ). A human Burkitt's B-lymphoma cell line, DND-39, and DND-39 cells transfected with the germ line ε promoter-luciferase gene (DND-39/Gε cells) were prepared and cultured, as described before (32, 33). HEK 293T cells were cultured in Dulbecco's modified Eagle's medium (Invitrogen) supplemented with 10% fetal calf serum, 100 μg/ml streptomycin, and 10 units/ml penicillin G.

Plasmids and Transfection—Plasmids encoding wild types of hIL-13Rα1 (pIRES1hyg-FLAG-hIL-13Rα1) and hIL-13Rα2 (pIRESneo2-HA-hIL-13Rα2) were prepared as described previously (32, 33). The FLAG and HA sequences were attached to the N termini of the D1 regions of hIL-13Rα1 and hIL-13Rα2 cDNA, respectively. The mutated types of IL-13Rα1 and IL-13Rα2 were generated by the QuikChange method (Stratagene, La Jolla, CA) or the modified inverse PCR method using mutation-incorporated oligonucleotides as the primers and pIRES1hyg-FLAG-hIL-13Rα1 and pIRESneo2-HA-hIL-13Rα2 as the templates.

[2] E. Honjo, unpublished data.

The plasmids were transfected into DND-39 cells by electroporation. Stable transfected cells were maintained with the culture medium containing 250 μg/ml hygromycin B (Wako, Osaka, Japan) for the hIL-13Rα1 mutants or 1.25 mg/ml G418 (Sigma) for the hIL-13Rα2 mutants, respectively. Expression of the receptors was confirmed by flow cytometry (FACSCalibre, BD Biosciences) using anti-FLAG antibodies (Abs, Sigma) for the IL-13Rα1 mutants and anti-HA Abs (Sigma) for the IL-13Rα2 mutants. Transient transfection of the plasmids into HEK 293T cells was performed by Lipofectamine 2000 (Invitrogen), according to the manufacturer's protocol.

Sequence Alignment and Homology Model Building—Alignment of the amino acid sequences of hIL-13Rα2 and hIL-13Rα1 without signal peptides (1 to 26, and 1 to 22, respectively) and prediction of FnIII domains (D1, D2, and D3), the transmembrane regions, and several β-strand sequences of the D2 and D3 domains of both receptors were executed through the MyHits data base (34). The sequence alignments of extracellular portions of human prolactin (PRL) receptor-hIL-13Rα2 and human gp130-hIL-13Rα1 were performed by FUGUE (35) with slight manual modification based on experimental results.

The complex structure of IL-13 and the D2 and D3 domains of hIL-13Rα2 was modeled based on the crystal structure of the GH·PRLR complex (PDB code 1BP3). The hIL-13Rα1 was modeled from the crystal structure of the viral IL-6·gp130 complex (PDB code 1I1R), and the resulting structure was overlaid onto the IL-13·hIL-13Rα2 complex structure model. Homology modelings of hIL-13Rα2 and hIL-13Rα1

were generated with MODELLER6v2 (36) followed by energy minimization and simulated annealing with Amber. The figures were drawn with DS Viewer Pro 5.0 (Accerlys, CA).

^{125}I-IL-13 Binding Assay—Iodination of IL-13 and the binding assay were performed as described previously (33). In brief, 1 μg of IL-13 and 1 mCi of $Na^{125}I$ in 50 μl of phosphate-buffered saline were incubated in a microcentrifuge tube coated with 2 μg of IODO-GEN (Pierce) at 4 °C for 10 min. Radiolabeled IL-13 was purified by a PD-10 column (Amersham Biosciences) and stored at 4 °C for up to 2 weeks. The concentration of ^{125}I-IL-13 was quantified by self-displacement of IL-13Rα2-expressing DND-39 cells. After cells were incubated with various concentrations of ^{125}I-IL-13 at 4 °C for 2 h, bound and free ligands were separated by centrifugation through an oil gradient, and their radioactivity was measured. Nonspecific binding was determined by counts in the presence of 100-fold unlabeled IL-13. The dissociation constants (K_d) were determined from specific binding data by using the program GraphPad Prism Version 4 (GraphPad Software, Inc., San Diego).

Luciferase Assay—The luciferase assay was performed as described previously (33). DND-39/Gε cells transfected with the mutated hIL-13Rα1 were stimulated with the indicated concentrations of IL-4 or IL-13 for 24 h, and then total cell lysates were applied to the Picagene Dual Luciferase assay kit (Toyo, Inc., Tokyo, Japan). HEK 293T cells were cotransfected with various types of pIRES1hyg-FLAG-hIL-13Rα1, pME18S-STAT6, and pGL3-N4x8 (kind gifts of Dr. T. Sugahara, Asahi Kasei Pharma Corp., Fuji, Japan). pGL3-N4x8 has the eight tandem-lined STAT6-responsible element (TTCNNNNGAA), as a promoter sequence of the firefly luciferase gene. The *Renilla* luciferase reporter gene (phRL-Tk; Promega, Madison, WI) was used as an internal control. 24 h after transfection, HEK 293T cells were detached by phosphate-buffered saline containing 5 mM EDTA, washed twice with phosphate-buffered saline, and reseeded. Adhered HEK 293T cells were stimulated with the indicated concentrations of IL-4 or IL-13 for 16 h, followed by washing once by phosphate-buffered saline, and total cell lysates were applied to the Picagene Dual Luciferase assay kit.

Western Blotting and Immunoprecipitation—The procedures of Western blotting and immunoprecipitation were performed as described previously (37). DND-39 cells stably transfected with various kinds of IL-13Rα1 were stimulated with 10 ng/ml IL-4 or IL-13 at 37 °C for 10 min. The solubilized lysates or the immunoprecipitates from the lysates with anti-TYK2 Ab (Santa Cruz Biotechnology, Santa Cruz, CA) were subjected to SDS-PAGE and transferred to polyvinylidene fluoride membrane. Membranes were incubated with either anti-FLAG Ab (Sigma), anti-HA Ab (Sigma), anti-phosphotyrosyl STAT6 Ab (Cell Signaling Technology, Inc., Beverly, MA), anti-STAT6 Ab (Santa Cruz Biotechnology), anti-phosphotyrosine Ab (4G10, Upstate Biotechnology, Lake Placid, NY) or anti-TYK2 Ab, followed by incubation with secondary Abs conjugated to horseradish peroxidase. The signals were visualized with an enhanced chemiluminescence system (ECL, Amersham Biosciences) and LAS-1000PLUS (Fuji Film, Tokyo, Japan).

RESULTS

Homology Modeling of the IL-13·hIL-13Rα2 Complex—In IL-13R, IL-13 binds to IL-13Rα1 primarily, and this complex is further stabilized by recruiting IL-4Rα, forming at least a trimer structure of ligand-receptor complex (4, 6). In contrast, IL-13Rα2 is likely to form a 1:1 complex with IL-13, which is easy to be modeled (11, 38). Therefore, we first built the homology modeling of the IL-13·hIL-13Rα2 complex. Because no structural information was available for the IL-13 receptors, the model was built based on the x-ray structure of the GH·PRLR 1:1 complex (PDB code 1BP3) as a template. Because PRLR does not contain an extra FnIII domain, we built the model as for the D2 and D3 domains of hIL-13Rα2, predicting that amino acids within the CRH of hIL-13Rα2 would interact with IL-13 (Fig. 2*A*). In this model, it was assumed that the E-F loop, the B′-C′ loop, and the F′-G′ loop of hIL-13Rα2 are composed of Leu-202 to Lys-208, Ser-259 to Arg-268, Asn-313 to Lys-328 amino acids, respectively (Fig. 1*B*). Furthermore, it was predicted that Tyr-207 in the E-F loop and Tyr-315 and Asp-318 in the F′-G′ loop of hIL-13Rα2 would be exposed to the binding interface (Figs. 1*A* and 2*A*). It is of note that Tyr-207 in the E-F loop of hIL-13Rα2 corresponds to Trp-72 of PRLR,

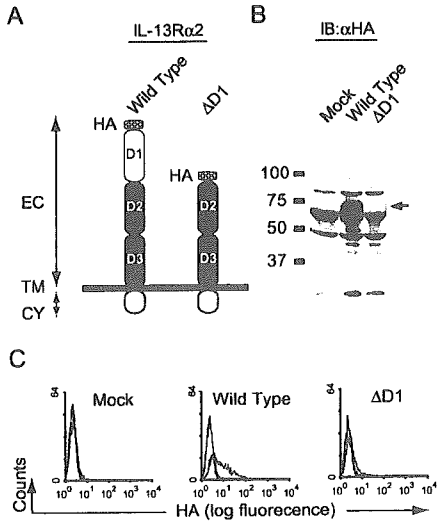

FIG. 4. **Expression of D1-deleted types of IL-13Rα2.** *A*, schematic model of D1-deleted type of hIL-13Rα2. *EC*, *TM*, and *CY* represent the extracellular domain, transmembrane domain, and cytoplasmic domain, respectively. Either wild type or the D1-deleted type of hIL-13Rα2 was transfected into HEK 293T cells. Their protein expression was analyzed by Western blotting (*B*) and flow cytometry (*C*). In *B*, the *arrow* represents the expressed hIL-13Rα2. In *C*, the *shaded* and *open areas* represent the counts with or without the first Ab, respectively.

Trp-104 of GHR, Phe-169 of gp130, and Phe-93 of the erythropoietin receptor, known as a "hot spot" of the ligand binding (Refs. 15, 16, 18, 39, and Fig. 1*B*).

Identification of Critical Residues of the D2 and D3 Domains of hIL-13Rα2 for Binding to IL-13—To address the importance of the amino acids in the D2 and D3 domains of hIL-13Rα2, predicted based on the homology modeling for binding of IL-13, we generated several kinds of hIL-13Rα2 mutated in these amino acids and analyzed their binding affinity for IL-13. We first analyzed the mutated hIL-13Rα2 in which Tyr-207, Asp-271, Tyr-315, and Asp-318 were replaced with Ala (4A-mut, Fig. 3*A*). In the modeling, Asp-271 on the strand C′ was assumed to locate close to Asp-318 (Fig. 2*A*). When 4A-mut was transfected into DND-39 cells, although the expression level of the receptor on the cell surface was invariable with that of the wild type of hIL-13Rα2 (Fig. 3*B*), no binding activity was detected (Fig. 3, *A* and *C*), demonstrating the critical roles of these four amino acids in binding to IL-13. To delineate the contribution of each of these four residues in binding to IL-13, we next analyzed the mutants in which Tyr-207, Asp-271, Tyr-315, or Asp-318 was replaced with Ala (Fig. 3*A*). When any of these four amino acids was mutated with Ala, the affinity of the mutated hIL-13Rα2 was significantly decreased. Expression of these four single mutated hIL-13Rα2 on the cell surface was invariable with the wild type (Fig. 3*B*). When Asp-318 was replaced with Ala together with Asp-271, the affinity was lowered more than in the single exchange of Asp-271 or Asp-318 (Fig. 3*A*). The replacement of amino acids that were either adjacent or close to these four critical amino acids (Asp-206, Ala-267, Arg-268, Ser-317, and Asp-319) affected the affinity with IL-13 (Fig. 3*A*). Double mutations of Glu-289 and Glu-291 with Ala, but not with Gln, slightly decreased the affinity, indicating that a hydrogen bond may be formed between Glu-289 and/or Glu-291 and IL-13. These results coincided with the molecular model in that the E-F loop and the F′-G′ loop of hIL-13Rα2 generates the main binding surface to IL-13 and that the critical amino acids in these loops (Tyr-207, Asp-271, Tyr-315, and Asp-318) are involved in comprising the binding interface at focal contacts. Particularly, it turned out that Tyr-207 is a hot spot for the ligand binding as well as Trp-72 of

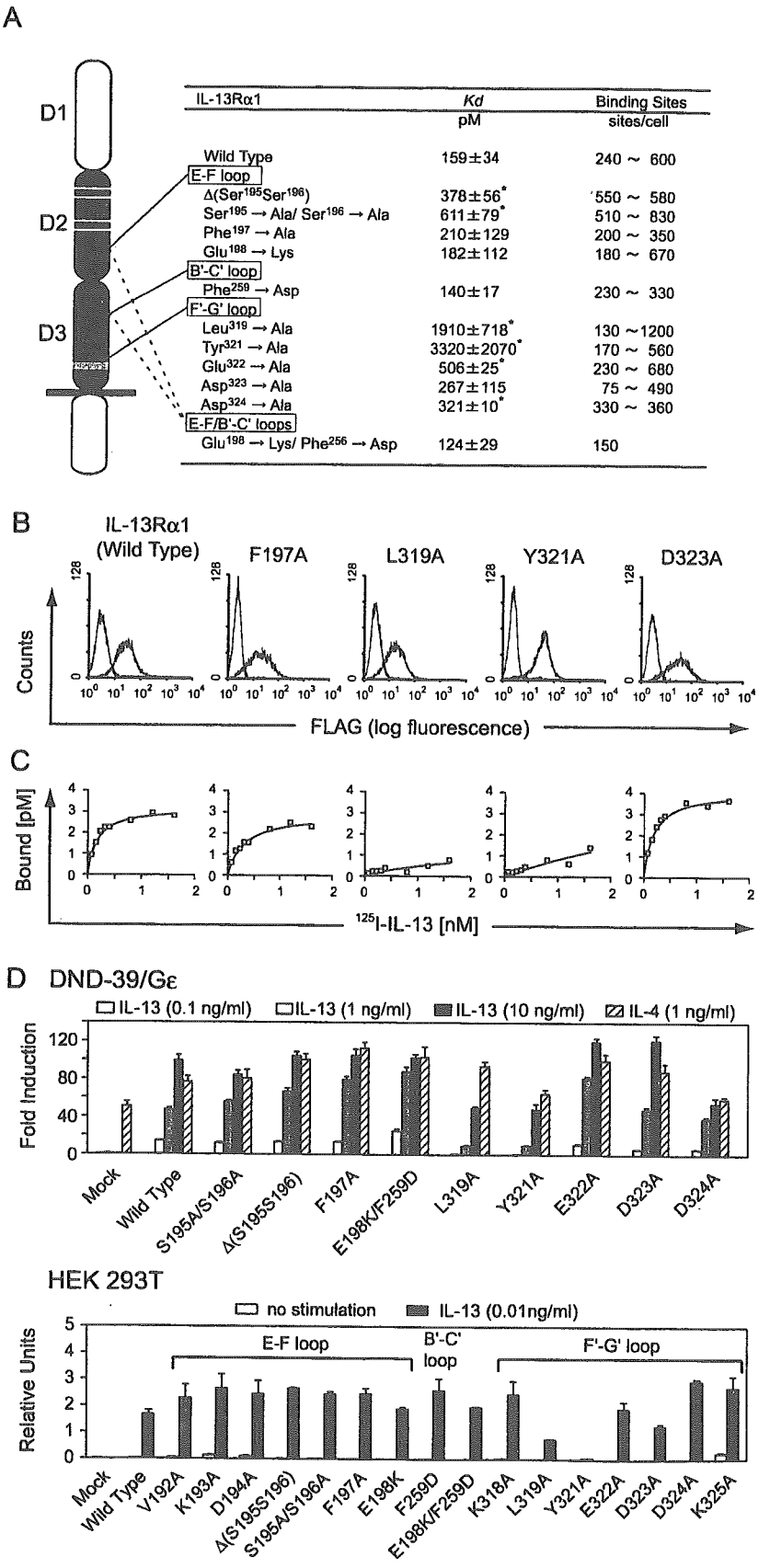

FIG. 5. **Characterization of the mutated types of hIL-13Rα1.** *A*, schematic model of mutated types of hIL-13Rα1 and their *Kd* values with IL-13 using stable DND-39 transfectants. Experiments were done at least twice for one clone in at least two different clones, and statistical differences with $p < 0.05$ (*) are indicated. The *white bands* in the D2 domain and the *gray band* in the D3 domain represent the conserved cysteine residues and the WSXWS sequence. *B*, expression of hIL-13Rα1 on the surface of DND-39/Gε cells stably transfected with hIL-13Rα1 (wild type, F197A, L319A, Y321A, D323A) by flow cytometry. The *shaded* and *open areas* represent the counts with or without the first Ab, respectively. *C*, binding assay of DND-39/Gε cells stably transfected with hIL-13Rα1 (wild type, F197A, L319A, Y321A, D323A). *D*, luciferase assays using DND-39/Gε cells or HEK 293T cells expressing wild and mutated types of hIL-13Rα1. The cells were stimulated with the indicated concentrations of IL-13 and 1 ng/ml of IL-4 for 24 h (DND-39/Gε cells) or 16 h (HEK 293T cells).

PRLR, Trp-104 of GHR, Phe-169 of gp130, and Phe-93 of the erythropoietin receptor. Although Asp-271 in the B'-C' loop is not exposed to the main binding interface, this amino acid would act cooperatively with Asp-318 for the binding.

Critical Role of the D1 Domain of hIL-13Rα2 in Its Expression—We next analyzed the functional role of the D1 domains of hIL-13Rα2, which could not be modeled because of a lack of information about homologous structure. For this purpose, we

generated a truncated type of hIL-13Rα2 lacking its D1 domain (hIL-13Rα2ΔD1, Fig. 4*A*). When hIL-13Rα2ΔD1 was transfected in HEK 293T cells, its expression was not detected by either Western blotting or flow cytometry analysis (Fig. 4, *B* and *C*). These results showed that the D1 domain of hIL-13Rα2 is critical for its expression.

Homology Modeling of the IL-13·hIL-13Rα1 Complex—Because the extracellular portions of IL-13Rα1 and IL-13Rα2 are homologous (Fig. 1*A*; ~33%) and several common amino acids in α-helix D of IL-13 are important for binding to both receptors (30), it is reasoned that amino acid residues involved in IL-13 binding are topologically conserved between these two receptors. We built a homology model of the IL-13·hIL-13Rα1 complex using the x-ray structures of the viral IL-6·gp130 complex (PDB code 1I1R) and the IL-13·hIL-13Rα2 modeling as templates (Fig. 2*B*). In this model, it was assumed that the E-F loop, the B′-C′ loop, and the F′-G′ loop are composed of Thr-190 to Glu-198, Glu-248 to Arg-256, and Asn-317 to Glu-333 amino acids, respectively (Fig. 1*C*). Furthermore, it was predicted that Phe-197 in the E-F loop would correspond to Tyr-207 of hIL-13Rα2 and that Leu-319 and Asp-323 in the F′-G′ loop would correspond to Tyr-315 and Asp-318 of hIL-13Rα2, respectively (Fig. 1*A*). The E-F loop of hIL-13Rα1 was two residues longer than that of hIL-13Rα2, and Ser-195 to Ser-196 was assumed to be the unique sequence to hIL-13Rα1 because no amino acid in hIL-13Rα2 corresponds to these amino acids (Fig. 1*A*).

Identification of Critical Residues of the D2 and D3 Domains of hIL-13Rα1 for Binding to IL-13—We explored whether the E-F loop and the F′-G′ loop of hIL-13Rα1 generate the main binding interface to IL-13 as well as hIL-13Rα2 and whether the amino acids in those loops of hIL-13Rα1 corresponding to the critical amino acids in hIL-13Rα2 contribute to the binding. To address this possibility, we generated several kinds of mutated hIL-13Rα1 and analyzed their binding affinity for IL-13. Because DND-39/Gε cells express endogenous hIL-4Rα, but not hIL-13Rα1, the mutated hIL-13Rα1 transfected on the cells comprises IL-13R/type II IL-4R together with endogenous hIL-4Rα (1). We first analyzed the involvement of the E-F loop of hIL-13Rα1 for binding to IL-13. When both Ser-195 and Ser-196, unique amino acids in hIL-13Rα1, were exchanged with Ala, the affinity was decreased, although the deleted mutant of both amino acids showed only a slight decrease (Fig. 5*A*). Mutations of Phe-197 corresponding to Tyr-207 in hIL-13Rα2 or adjacent Glu-198 did not show any difference. We next analyzed the involvement of the F′-G′ loop. When either Leu-319 or Asp-323 corresponding to Tyr-315 and Asp-318 in hIL-13Rα2 was replaced with Ala, the affinity of the mutated hIL-13Rα1 to IL-13 was dramatically decreased in L319A, but there was no change in D323A (Fig. 5, *A* and *C*). Replacement of Asp-324 adjacent to Asp-323 showed only a slight decrease of the affinity. In contrast, when Tyr-321 was exchanged with Ala, the affinity was decreased significantly. Replacement of Glu-322 also attenuated the affinity, but less than Leu-319 or Tyr-321. Expression of these mutated types of hIL-13Rα1 was invariable with the wild type (Fig. 5*B* and data not shown). Substitution at Phe-259 corresponded to Asp-271 in hIL-13Rα2 on the strand C′ and did not influence the affinity.

We next tested whether the lowered affinities of the mutated hIL-13Rα1 would lead to reduction in the IL-13 signal. DND-39/Gε cells expressing endogenous hIL-4Rα and the transfected hIL-13Rα1 are able to transduce the IL-13 signal by engagement of the ligand, augmenting expression of the reporter gene. When we performed a reporter gene assay using DND-39/Gε cells expressing all kinds of the mutated hIL-13Rα1 investigated for the binding assay, only the mutant types of Leu-319 and Tyr-321 significantly impaired the IL-13 response (Fig. 5*D* and data not shown). The double mutation type at Ser-195 and Ser-196 and the single mutation types at Glu-322 or Asp-324 showed normal IL-13 responses. The responses of all transfectants to IL-4 were invariable. To identify the amino acid residues critical for binding to hIL-13Rα1, we generated five more mutants and analyzed their IL-13 responses in HEK 293T cells. In this experiment, we stimulated HEK 293T cells with 0.01 ng/ml IL-13 in which expression of the reporter gene through transfected hIL-13Rα1, but not endogenous hIL-13Rα1, was detected (Fig. 5*D*). We confirmed that the responses to IL-13 could be detected as the same as in the system using DND-39/Gε cells and that again L319A and Y321A showed lower activities. However, none of the additionally investigated mutants, single mutations of Val-192, Lys-193, or Asp-194 in E-F loop and Lys-318 or Lys-325 in F′-G′ loop with Ala, changed the IL-13 responses. These results suggested that both the E-F loop and more dominantly the F′-G′ loop contribute to binding to IL-13 in hIL-13Rα1 as well as hIL-13Rα2 and that particularly, Leu-319 and Tyr-321 in the F′-G′ loop are critical residues for the binding to transduce the IL-13 signal. Leu-319 in hIL-13Rα1 corresponding to Tyr-315 in hIL-13Rα2 is a positionally conserved hydrophobic residue for binding to IL-13.

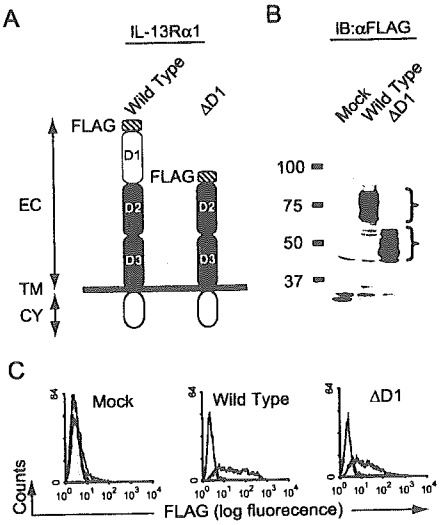

FIG. 6. **Expression of D1-deleted types of IL-13Rα1.** *A*, schematic model of D1-deleted type of hIL-13Rα1. Either wild type or the D1-deleted type of hIL-13Rα1 was transfected into HEK 293T cells. Their protein expression was analyzed by Western blotting (*B*) and flow cytometry (*C*). In *B*, *braces* represent the expressed hIL-13Rα1. In *C*, the *shaded* and *open areas* represent the counts with or without the first Ab, respectively.

Critical Role of the D1 Domain of hIL-13Rα1 in Its Binding to IL-13 but Not to IL-4—We next analyzed the functional role of the D1 domain of hIL-13Rα1, which could not be modeled because of a lack of information about homologous structure as well as hIL-13Rα2. For this purpose, we generated a truncated type of hIL-13Rα1 lacking its D1 domain (hIL-13Rα1ΔD1; Fig. 6*A*). When hIL-13Rα1ΔD1 was transfected in HEK 293T cells, its expression was detected by both Western blotting and flow cytometry analysis at the same level as the wild type in contrast to hIL-13Rα2ΔD1, confirming the ability of this mutated type to be expressed on the cell surface (Fig. 6, *B* and *C*).

We next analyzed the involvement of the D1 domain of hIL-13Rα1 in binding to IL-13. hIL-13Rα1ΔD1 completely lost the binding affinity to IL-13, although it was expressed on the cell surface at the same level as the wild type (Fig. 7, *A* and *B*). In concordance with the results of the binding assay, hIL-13Rα1ΔD1 failed to induce the transcription of the reporter

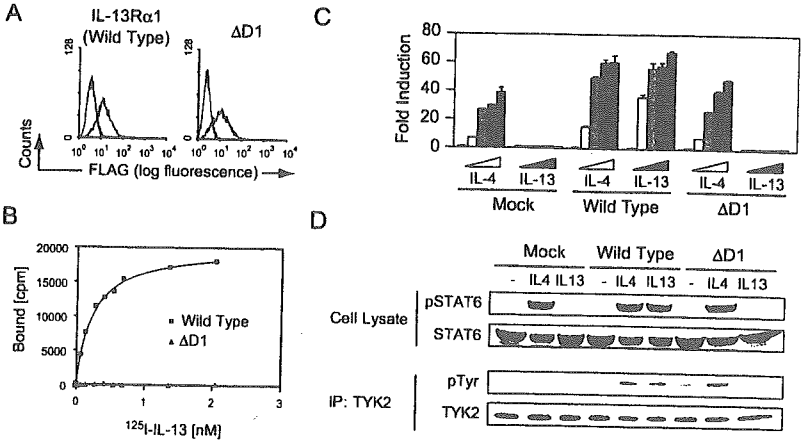

FIG. 7. **Signal transduction of D1-deleted type of IL-13Rα1.** *A*, expression of the wild and D1-deleted types of hIL-13Rα1 on the surface of stable DND-39/Gε transfectants by flow cytometry. The *shaded* and *open areas* represent the count with or without the first Ab, respectively. *B*, the specific bindings of ^{125}I-IL-13 to DND-39/Gε cells stably transfected with the wild (*squares*) and D1-deleted (*triangles*) types of hIL-13Rα1. *C*, luciferase assay using DND-39/Gε cells expressing wild and D1-deleted types of hIL-13Rα1. The cells were stimulated with IL-4 or IL-13 (0, 0.1, 0.4, 1, and 10 ng/ml) for 24 h. *D*, activation of STAT6 and TYK2 using DND-39/Gε cells expressing wild and D1-deleted types of hIL-13Rα1. The cells were stimulated with 10 ng/ml IL-4 or IL-13 for 10 min.

gene and activate both STAT6 and TYK2 by engagement of IL-13 (Fig. 7, *C* and *D*). In contrast, expression of hIL-13Rα1ΔD1 did not prevent the reporter gene activity or STAT6 activation by IL-4 (Fig. 7, *C* and *D*). IL-4 could activate STAT6 through either type I IL-4R composed of IL-4Rα and the common γ chain (γc) or type II IL-4R composed of IL-4Rα and IL-13Rα1. It would be possible that even though the type II IL-4R composed of IL-4Rα and hIL-13Rα1ΔD1 was nonfunctional, IL-4 could activate STAT6 through the type I IL-4R. However, activation of TYK2, a specific signaling event of type II IL-4R/IL-13R, was detected, when hIL-13Rα1ΔD1-expressed cells were stimulated with IL-4 (Fig. 7*D*), indicating that the type II IL-4R composed of hIL-4Rα and hIL-13Rα1ΔD1 was functional for the IL-4 binding and its signaling. These results suggested that the D1 domain of hIL-13Rα1 is critical for binding to IL-13, but not to IL-4.

DISCUSSION

In this article, we identified for the first time critical residues in the CRHs of hIL-13Rα1 and hIL-13Rα2 in binding to IL-13 by the mutagenesis approach based on homology modeling of the IL-13·hIL-13 receptor complexes. In our findings, Tyr-207, Asp-271, Tyr-315, and Asp-318 in the CRH of hIL-13Rα2, and Leu-319 and Tyr-321 in the CRH of hIL-13Rα1 are critical residues for binding to IL-13 (Figs. 3 and 5). Leu-319 in hIL-13Rα1 and Tyr-315 in hIL-13Rα2 are positionally conserved hydrophobic amino acids. Tyr-207, Tyr-315, and Asp-318 in hIL-13Rα2, and Leu-319 in hIL-13Rα1 are conserved in all known species, whereas Tyr-321 in hIL-13Rα1 is conserved in porcine and canine IL-13Rα1 but is replaced by Phe in rat and mouse IL-13Rα1. It has been assumed that the binding site on IL-13 to IL-13Rα1 is α-helix A and α-helix D because the α-helix A and α-helix D of IL-4 interact with either γc or IL-13Rα1, based on the structure of the IL-4·IL-4Rα complex (20), and IL-13 has a significant similarity in folding topology with IL-4 (40, 41). Consistent with this assumption, it has been demonstrated that several amino acid residues in α-helix D of IL-13 (Lys-90, Ile-91, His-103, Leu-104, Lys-105, Lys-106, Arg-109, Glu-110, and Arg-112) are important for binding to hIL-13Rα1 and/or hIL-13Rα2, although α-helix A of IL-13 is predicted to interact with IL-4Rα (29–31). Some of these amino acids would interact with those identified in our present study, involved in the binding between IL-13 and hIL-13Rα1/hIL-13Rα2. It is of note that Asp-318 of hIL-13Rα2, contributing most to the binding among the investigated amino acid residues, was assumed to interact with Lys-105 of IL-13, forming a salt bridge, in our present model (data not shown).

We furthermore demonstrated that the D1 domain is necessary for expression of hIL-13Rα2, but not for that of hIL-13Rα1

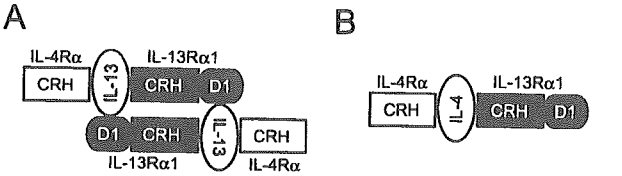

FIG. 8. **Schematic model of the hexamer of the IL-13·IL-13Rα1·IL-4Rα complex.** IL-13 may form a trimer by binding to the CRH composed of the D2 and D3 domains and furthermore forms a hexamer by binding to the D1 domain in the opposite trimer (*A*), whereas IL-4 forms a trimer by binding to CRHs of IL-13Rα1 and IL-4Rα (*B*).

(Figs. 4 and 6), whereas the D1 domain of hIL-13Rα1 is critical for binding to IL-13 (Fig. 7). Thus far, it is unclear how the D1 domain of hIL-13Rα2 is involved in the expression mechanism of the receptor. When the D1 domain is deleted, the D2/D3 domains of hIL-13Rα2 may be unable to keep their conformations. Mutagenesis analyses of the extra FnIII domain have already shown its importance in binding to ligands and the signal transduction in gp130 (21, 22), G-CSFR (23, 24), LIFR (25, 26), and IL-5Rα (27). Our present finding is the first evidence showing involvement of the D1 domain of hIL-13Rα1 in binding to IL-13. Structural analyses of the IL-6·IL-6Rα·gp130 complex show that this complex is a 2:2:2 hexamer, in which the extra FnIII domains interact with the binding epitopes on IL-6 in the opposite trimers (18, 28). Although the precise structure of the IL-13·hIL-13Rα1·hIL-4Rα complex remains undetermined, this complex may also form a 2:2:2 hexamer via the D1 domain of hIL-13Rα1 (Fig. 8*A*).

We found that the D1 domain of hIL-13Rα1 is critical for the binding and signal transduction of IL-13, but not IL-4 (Fig. 7). This finding suggests that the binding modes of IL-4 and IL-13 with IL-13Rα1 are different, although both ligands utilize the common heterodimeric complex composed of IL-4Rα and IL-13Rα1. Similarly, it has been already shown that the D1 domain of gp130 is needed for binding to IL-6, but not to LIF, IL-11, ciliary neurotrophic factor, or oncostatin-M (21, 42). IL-4 first binds to IL-4Rα and then recruits IL-13Rα1 or γc to the complex, forming the high affinity receptor. IL-13Rα1 alone has almost no binding activity to IL-4 (4, 43). Mutagenesis experiments have suggested that Arg-121 and Tyr-124 located at the α-helix D of IL-4 are important for the interaction with IL-13Rα1 (44, 45), which overlaps with the interaction site to γc (46, 47). Our present finding indicates that α-helix D of IL-4 probably interacts with the D2 and D3 domains of IL-13Rα1, independently from its D1 domain (Fig. 8*B*). Involvement of the D1 domain of hIL-13Rα1 in binding to IL-13, but not to IL-4, at

least partially explains the different affinities of hIL-13Rα1 to IL-13 and IL-4.

We found previously that there exists a variant of the *IL13* gene, in which arginine residue at 110 (Arg-110; numbering from the starting residue of the mature protein at Gly-1) is replaced by glutamine (Gln-110); this variant is associated with bronchial asthma in both Japanese and British populations (48). The same variant was thereafter reported to be positively correlated with high IgE levels and atopic dermatitis (49–51). We furthermore demonstrated that the Gln-110 type has a lower affinity with hIL-13Rα2 than the Arg-110 type, whereas both types show the same affinity with hIL-13Rα1, which would cause up-regulation of the IL-13 concentration in the body (33). We assumed that the interaction between Arg-110 and hIL-13Rα2 might be disrupted by the substitution of the glutamine residue, although the alanine scanning approach showed only a slight involvement of this residue in binding to hIL-13Rα2 (30). If such an amino acid in hIL-13Rα2 interacting with Arg-110 in IL-13 were displaced by another amino acid, the affinities of the mutant hIL-13Rα2 with the Arg-110 and Gln-110 types would become the same. All of the investigated mutant hIL-13Rα2 showed lower affinities with the Gln-110 type than the Arg-110 type or the wild type (data not shown). These results implied the possibility that R110Q may change the conformation of IL-13 itself, not the direct interaction with IL-13Rα2.

Considering the importance of IL-13 in the pathogenesis of allergic diseases, particularly bronchial asthma, several IL-13 antagonists have been developed as means of improving allergic states (1). Our present finding would be useful in these strategies. The D1 domain is a particularly good target to develop a neutralizing Ab or a low molecular weight compound to block specifically the interaction between hIL-13Rα1 and IL-13, but not IL-4. It has been already shown that the monoclonal Abs against the D1 domains of gp130 (21, 22, 42) or G-CSFR (24) inhibit binding to ligands and their signals. It will be of great interest to analyze the effects of a neutralizing Ab or a low molecular weight compound targeting the D1 domain of IL-13Rα1 on the development of allergic diseases.

In conclusion, we for the first time identified the critical residues in the CRH of hIL-13Rα1 and hIL-13Rα2 for binding to IL-13 and clarified the roles of the D1 domains of these receptors by the mutagenesis approach. These results provide the basis for a precise understanding of the interaction between IL-13 and its receptors.

Acknowledgment—We thank Dr. Dovie R. Wylie for a critical review of this manuscript.

REFERENCES

1. Izuhara, K., and Arima, K. (2004) *Drug News Perspect.* **17,** 91–98
2. Wills-Karp, M., and Chiaramonte, M. (2003) *Curr. Opin. Pulm. Med.* **9,** 21–27
3. Wynn, T. A. (2003) *Annu. Rev. Immunol.* **21,** 425–456
4. Aman, M. J., Tayebi, N., Obiri, N. I., Puri, R. K., Modi, W. S., and Leonard, W. J. (1996) *J. Biol. Chem.* **271,** 29265–29270
5. Miloux, B., Laurent, P., Bonnin, O., Lupker, J., Caput, D., Vita, N., and Ferrara, P. (1997) *FEBS Lett.* **401,** 163–166
6. Andrews, A. L., Holloway, J. W., Puddicombe, S. M., Holgate, S. T., and Davies, D. E. (2002) *J. Biol. Chem.* **277,** 46073–46078
7. Kelly-Welch, A. E., Hanson, E. M., Boothby, M. R., and Keegan, A. D. (2003) *Science* **300,** 1527–1528
8. Caput, D., Laurent, P., Kaghad, M., Lelias, J., Lefort, S., Vita, N., and Ferrara, P. (1996) *J. Biol. Chem.* **271,** 16921–16926
9. Donaldson, D. D., Whitters, M. J., Fitz, L. J., Neben, T. Y., Finnerty, H., Henderson, S. L., O'Hara, R. M. J., Beier, D. R., Turner, K. J., Wood, C. R., and Collins, M. (1998) *J. Immunol.* **161,** 2317–2324
10. Bernard, J., Treton, D., Vermot-Desroches, C., Boden, C., Horellou, P., Angevin, E., Galanaud, P., Wijdenes, J., and Richard, Y. (2001) *Lab. Invest.* **81,** 1223–1231
11. Yasunaga, S., Yuyama, N., Arima, K., Tanaka, H., Toda, S., Maeda, M., Matsui, K., Goda, C., Yang, Q., Sugita, Y., Nagai, H., and Izuhara, K. (2003) *Cytokine* **24,** 293–303
12. Wood, N., Whitters, M. J., Jacobson, B. A., Witek, J., Sypek, J. P., Kasaian, M., Eppihimer, M. J., Unger, M., Tanaka, T., Goldman, S. J., Collins, M., Donaldson, D. D., and Grusby, M. J. (2003) *J. Exp. Med.* **197,** 703–709
13. Chiaramonte, M. G., Mentink-Kane, M., Jacobson, B. A., Cheever, A. W., Whitters, M. J., Goad, M. E., Wong, A., Collins, M., Donaldson, D. D., Grusby, M. J., and Wynn, T. A. (2003) *J. Exp. Med.* **197,** 687–701
14. Bazan, J. F. (1990) *Proc. Natl. Acad. Sci. U. S. A.* **87,** 6934–6938
15. Somers, W., Ultsch, M., De Vos, A. M., and Kossiakoff, A. A. (1994) *Nature* **372,** 478–481
16. Syed, R. S., Reid, S. W., Li, C., Cheetham, J. C., Aoki, K. H., Liu, B., Zhan, H., Osslund, T. D., Chirino, A. J., Zhang, J., Finer-Moore, J., Elliott, S., Sitney, K., Katz, B. A., Matthews, D. J., Wendoloski, J. J., Egrie, J., and Stroud, R. M. (1998) *Nature* **395,** 511–516
17. Aritomi, M., Kunishima, N., Okamoto, T., Kuroki, R., Ota, Y., and Morikawa, K. (1999) *Nature* **401,** 713–717
18. Chow, D., He, X., Snow, A. L., Rose-John, S., and Garcia, K. C. (2001) *Science* **291,** 2150–2155
19. Yoon, C., Johnston, S. C., Tang, J., Stahl, M., Tobin, J. F., and Somers, W. S. (2000) *EMBO J.* **19,** 3530–3541
20. Hage, T., Sebald, W., and Reinemer, P. (1999) *Cell* **97,** 271–281
21. Hammacher, A., Richardson, R. T., Layton, J. E., Smith, D. K., Angus, L. J., Hilton, D. J., Nicola, N. A., Wijdenes, J., and Simpson, R. J. (1998) *J. Biol. Chem.* **273,** 22701–22707
22. Kurth, I., Horsten, U., Pflanz, S., Dahmen, H., Kuster, A., Grotzinger, J., Heinrich, P. C., and Muller-Newen, G. (1999) *J. Immunol.* **162,** 1480–1487
23. Fukunaga, R., Ishizaka-Ikeda, E., Pan, C. X., Seto, Y., and Nagata, S. (1991) *EMBO J.* **10,** 2855–2865
24. Layton, J. E., Hall, N. E., Connell, F., Venhorst, J., and Treutlein, H. R. (2001) *J. Biol. Chem.* **276,** 36779–36787
25. Bitard, J., Daburon, S., Duplomb, L., Blanchard, F., Vuisio, P., Jacques, Y., Godard, A., Heath, J. K., Moreau, J. F., and Taupin, J. L. (2003) *J. Biol. Chem.* **278,** 16253–16261
26. Plun-Favreau, H., Perret, D., Diveu, C., Froger, J., Chevalier, S., Lelievre, E., Gascan, H., and Chabbert, M. (2003) *J. Biol. Chem.* **278,** 27169–27179
27. Ishino, T., Pasut, G., Scibek, J., and Chaiken, I. (2004) *J. Biol. Chem.* **279,** 9547–9556
28. Boulanger, M. J., Chow, D. C., Brevnova, E. E., and Garcia, K. C. (2003) *Science* **300,** 2101–2104
29. Thompson, J. P., and Debinski, W. (1999) *J. Biol. Chem.* **274,** 29944–29950
30. Madhankumar, A. B., Mintz, A., and Debinski, W. (2002) *J. Biol. Chem.* **277,** 43194–43205
31. Oshima, Y., and Puri, R. K. (2001) *J. Biol. Chem.* **276,** 15185–15191
32. Umeshita-Suyama, R., Sugimoto, R., Akaiwa, M., Arima, K., Yu, B., Wada, M., Kuwano, M., Nakajima, K., Hamasaki, N., and Izuhara, K. (2000) *Int. Immunol.* **12,** 1499–1509
33. Arima, K., Umeshita-Suyama, R., Sakata, Y., Akaiwa, M., Mao, X. Q., Enomoto, T., Dake, Y., Shimazu, S., Yamashita, T., Sugawara, N., Brodeur, S., Geha, R., Puri, R. K., Sayegh, M. H., Adra, C. N., Hamasaki, N., Hopkin, J. M., Shirakawa, T., and Izuhara, K. (2002) *J. Allergy Clin. Immunol.* **109,** 980–987
34. Pagni, M., Ioannidis, V., Cerutti, L., Zahn-Zabal, M., Jongeneel, C. V., and Falquet, L. (2004) *Nucleic Acids Res.* **32,** 332–335
35. Shi, J., Blundell, T. L., and Mizuguchi, K. (2001) *J. Mol. Biol.* **310,** 243–257
36. Sali, A., and Blundell, T. L. (1993) *J. Mol. Biol.* **234,** 779–815
37. Izuhara, K., Heike, T., Otsuka, T., Yamaoka, K., Mayumi, M., Imamura, T., Niho, Y., and Harada, N. (1996) *J. Biol. Chem.* **271,** 619–622
38. Feng, N., Lugli, S. M., Schnyder, B., Gauchat, J., Graber, P., Schlagenhauf, E., Schnarr, B., Wiederkehr-Adam, M., Duschl, A., Heim, M. H., Lutz, R. A., and Moser, R. (1998) *Lab. Invest.* **78,** 591–602
39. Clackson, T., and Wells, J. A. (1995) *Science* **267,** 383–386
40. Moy, F. J., Diblasio, E., Wilhelm, J., and Powers, R. (2001) *J. Mol. Biol.* **310,** 219–230
41. Eisenmesser, E. Z., Horita, D. A., Altieri, A. S., and Byrd, R. A. (2001) *J. Mol. Biol.* **310,** 231–241
42. Wijdenes, J., Heinrich, P. C., Muller-Newen, G., Roche, C., Gu, Z. J., Clement, C., and Klein, B. (1995) *Eur. J. Immunol.* **25,** 3474–3481
43. Hilton, D. J., Zhang, J. G., Metcalf, D., Alexander, W. S., Nicola, N. A., and Willson, T. A. (1996) *Proc. Natl. Acad. Sci. U. S. A.* **93,** 497–501
44. Shanafelt, A. B., Forte, C. P., Kasper, J. J., Sanchez-Pescador, L., Wetzel, M., Gundel, R., and Greve, J. M. (1998) *Proc. Natl. Acad. Sci. U. S. A.* **95,** 9454–9458
45. Schnarr, B., Ezernieks, J., Sebald, W., and Duschl, A. (1997) *Int. Immunol.* **9,** 861–868
46. Kruse, N., Shen, B.-J., Arnold, S., Tony, H.-P., Müller, T., and Sebald, W. (1993) *EMBO J.* **12,** 5121–5129
47. Letzelter, F., Wang, Y., and Sebald, W. (1998) *Eur. J. Biochem.* **257,** 11–20
48. Heinzmann, A., Mao, X. Q., Akaiwa, M., Kreomer, R. T., Gao, P. S., Ohshima, K., Umeshita, R., Abe, Y., Braun, S., Yamashita, T., Roberts, M. H., Sugimoto, R., Arima, K., Arinobu, Y., Yu, B., Kruse, S., Enomoto, T., Dake, Y., Kawai, M., Shimazu, S., Sasaki, S., Adra, C. N., Kitaichi, M., Inoue, H., Yamauchi, K., Tomichi, N., Kurimoto, F., Hamasaki, N., Hopkin, J. M., Izuhara, K., Shirakawa, T., and Deichmann, K. A. (2000) *Hum. Mol. Genet.* **9,** 549–559
49. Graves, P. E., Kabesch, M., Halonen, M., Holberg, C. J., Baldini, M., Fritzsch, C., Weiland, S. K., Erickson, R. P., von Mutius, E., and Martinez, F. D. (2000) *J. Allergy Clin. Immunol.* **105,** 506–513
50. Liu, X., Nickel, R., Beyer, K., Wahn, U., Ehrlich, E., Freidhoff, L. R., Bjorksten, B., Beaty, T. H., and Huang, S. K. (2000) *J. Allergy Clin. Immunol.* **106,** 167–170
51. Leung, T. F., Tang, N. L., Chan, I. H., Li, A. M., Ha, G., and Lam, C. W. (2001) *Clin. Exp. Allergy* **31,** 1515–1521

Squamous cell carcinoma–related antigen in children with acute asthma

Natsuko Nishi, MD*; Michiko Miyazaki, MD*; Kosuke Tsuji, MD*; Tomohiro Hitomi, MD*; Eriko Muro, MD*; Masafumi Zaitsu, MD*; Syuichi Yamamoto, MD*; Shigeyasu Inada, MD*; Ikuko Kobayashi, MD*; Tomohiro Ichimaru, MD*; Kenji Izuhara, MD†; Fumio Nagumo, BS‡; Noriko Yuyama, PhD§; and Yuhei Hamasaki, MD*

Background: Increased serum levels of squamous cell carcinoma–related antigen (SCCA) have been observed in patients with allergic disorders, such as atopic dermatitis and bronchial asthma. T_H2 cytokines, which are known to be involved in the pathogenesis of allergic disorders, stimulate new synthesis of SCCA in cultured human airway epithelial cells.

Objective: To investigate whether SCCA levels increase during acute exacerbations of asthma in children and whether the T_H2 cytokines, interleukin 4 (IL-4) and IL-13, are associated with SCCA levels.

Methods: Serum levels of SCCA, IL-4, and IL-13 were measured by enzyme immunoassay during the acute phase of an asthma exacerbation (on hospital admission) and in the recovery phase (after symptoms had subsided).

Results: In the 35 children who participated in this study, serum levels of SCCA were significantly elevated in the acute phase (mean ± SD, 3.09 ± 2.03 ng/mL) compared with the recovery phase (mean ± SD, 1.47 ± 0.64 ng/mL) of an asthma exacerbation ($P < .001$). In 12 children, the IL-13 levels were observed to correlate with SCCA levels during the recovery phase ($r = 0.68$, $P = .02$) but not during the acute phase of an asthma exacerbation.

Conclusions: Serum SCCA levels increase during the acute phase of an asthma exacerbation. During this phase, the increased synthesis of SCCA is not associated with IL-13 but rather mediated by other undefined stimuli. IL-13 may contribute to the basal production of SCCA in asthmatic children.

Ann Allergy Asthma Immunol. 2005;94:391–397.

INTRODUCTION

The tumor marker squamous cell carcinoma–related antigen (SCCA) was originally purified from human uterine cervical squamous cell carcinoma cells.[1] Two types of SCCA (1 and 2) have been identified. Both of them are closely related serine protease inhibitors that belong to the ovalbumin-serpin families. The genes locate at 18q21 as a tandem duplication form, and the protein molecules number 45,000.[2] Following its discovery, SCCA expression was observed in normal epithelial cells from tissue, including the esophagus, tongue, and airways.[3] SCCA is released into the serum and can be measured using an enzyme immunoassay,[4] although it has a short half-life. Elevated serum concentrations of SCCA have been reported in several benign disorders, including allergic diseases such as atopic dermatitis.[5] Significantly greater serum SCCA levels have been observed in asthmatic children compared with nonasthmatic controls.[6] An increased production of SCCA has been observed in cultured airway epithelial cells following stimulation with the T_H2 cytokines interleukin 4 (IL-4) and IL-13.[6]

In this study, we measured the serum levels of SCCA in children with bronchial asthma during the acute and recovery phases of an exacerbation. We also measured the serum levels of IL-4, IL-13, and interferon-γ (IFN-γ) in some patients, after which we evaluated the relationship between each of these cytokines and SCCA. We further examined the data to see if there might be a correlation among serum SCCA levels, clinical symptoms, and laboratory data, such as atopic skin lesion and the level of serum IgE.

METHODS

From June 2001 to May 2002, children hospitalized in an affiliated hospital of Saga Medical School, Saga City, Japan, with acute exacerbations of bronchial asthma were investigated. The diagnosis of asthma was made based on (1) effectiveness to inhaled β-agonist, (2) history of recurrent dyspnea attacks, (3) increased serum IgE levels, and (4) family history of allergic diseases. Duration of disease indicates the time span since the patients were first diagnosed by pediatricians as having bronchial asthma. The patients who needed to be hospitalized because of moderate or severe asthma attacks were enrolled in the study. Levels of patients' asthma severity in daily life, defined according to the Global Initiative for Asthma, were classified as mild persistent or moderate persistent (Table 1). As a control group for the measurement of SCCA levels, 21 age-matched (mean ± SD,

* Department of Pediatrics, Faculty of Medicine, Saga University, Saga City, Japan.
† Department of Biochemistry, Faculty of Medicine, Saga University, Saga City, Japan.
‡ Department of Laboratory Medicine, Faculty of Medicine, Saga University, Saga City, Japan.
§ Gennox Research Inc, Tokyo, Japan.
Received for publication May 18, 2004.
Accepted for publication in revised form September 13, 2004.

Table 1. Patient Disease Profiles

Patient No./ sex/age	Duration of disease y	IgE, IU	Positive RAST result	Regular medication	Intravenous steroids	Severity of asthma	Severity of attack
1/F/4 y 3 m	0.75	1,715	MT, HD	TE, LT, and OBA		Mild persistent	Moderate
2/M/2 y 7 m	2	1,035	MT, HD, AN, FD	TE and OBA		Mild persistent	Moderate
3/F/3 y 4 m	0.5			TE and OBA		Mild persistent	Moderate
4/M/4 y 2 m	3	54	MT, HD	TE and OBA		Mild persistent	Moderate
5/M/6 y	4	403	MT, HD, AN	LT		Mild persistent	Moderate
6/M/11 y 5 m	8	498	MT, HD	TE, LT, and OBA	+	Mild persistent	Severe
7/M/8 y 11 m	2	10,535	MT, HD, FD	TE and LT	+	Mild persistent	Severe
8/M/2 y 3 m	1	275	MT, HD, FD	TE and OBA	+	Mild persistent	Severe
9/M 2 y 1 m	1	336	HD, FD	TE, LT, and OBA	+	Mild persistent	Severe
10/M/1 y 8 m	0.1	138	HD	TE, LT, and OBA	+	Mild persistent	Severe
11/M/4 y 7 m	3	290	MT, HD, AN	TE, LT, and OBA	+	Mild persistent	Severe
12/M/6 y 6 m	1	292	MT, HD	TE, LT, and OBA	+	Mild persistent	Severe
13/M/10 y 11 m	0.5	91	MT, HD	TE, LT, and OBA	+	Mild persistent	Severe
14/M/3 y 3 m	1	1,294	MT, AN	TE and LT	+	Mild persistent	Severe
15/M/5 y 8 m	4	120		TE, LT, and OBA		Moderate persistent	Moderate
16/M/2 y 1 m	0.5	222	FD	TE, LT, and OBA		Moderate persistent	Moderate
17/M/7 y 4 m	4			TE, LT, and OBA		Moderate persistent	Moderate
18/M/3 y 9 m	1	109	MT, HD	TE, LT, and OBA		Moderate persistent	Moderate
19/F/12 y 8 m	8	35		ICS		Moderate persistent	Moderate
20/M/7 y 2 m	1.5	442	MT, HD	TE, LT, OBA, and ICS	+	Moderate persistent	Severe
21/F/1 y 9 m	1	9		TE, LT, OBA, and ICS	+	Moderate persistent	Severe
22/M/2 y 10 m	2	412	MT, HD	TE, OBA, and ICS	+	Moderate persistent	Severe
23/M/1 y 5 m	0.8	222	FD	TE, LT, and OBA	+	Moderate persistent	Severe
24/F/5 y 9 m	6	5,393	MT, HD, AN	TE, LT, and ICS	+	Moderate persistent	Severe
25/M/5 y 4 m	4	38	MT, HD	TE, OBA, and ICS	+	Moderate persistent	Severe
26/M/10 m	0.5	19	AN, FD	TE, LT, and OBA	+	Moderate persistent	Severe
27/M/1 y 8 m	0			OBA		ND	Moderate
28/M/7 y 6 m	0	445	MT, HD	TE and OBA		ND	Moderate
29/F/9 y 8 m	5	1,729	MT, HD	TE		Mild persistent	Moderate
30/M/2 y 7 m	1			TE		Mild persistent	Moderate
31/M/3 y 5 m	1.5	941	MT, HD	TE and OBA	+	Mild persistent	Severe
32/F/14 y 6 m	11	226	HD, AN	TE, LT, OBA, and ICS		Moderate persistent	Moderate
33/F/4 y 6 m	3	95		TE and ICS		Moderate persistent	Moderate
34/M/3 y 3 m	2			TE and OBA		Moderate persistent	Moderate
35/F/11 m	0	12		TE and OBA	+	ND	Severe

Abbreviations: AN, animal; FD, food; HD, housedust; ICS, inhaled corticosteroid; LT, leukotriene modifier; MT, mite; ND, not determined; OBA, oral β-agonist; plus sign, positive; RAST, radioallergosorbent test; TE, theophylline.

5.71 ± 0.86 years), healthy children were enrolled after informed consent was obtained.

We measured patients' serum SCCA levels at the time of admission (ie, during the acute phase of their asthma exacerbation, when they showed signs of dyspnea and marked wheezing and their oxygen saturation as measured by pulse oximetry was <95% within 24 hours from the onset of the attack) and after their symptoms had subsided (ie, during the recovery phase, when they had no signs of dyspnea, wheezing was either present or absent, and their oxygen saturation as measured by pulse oximetry was >96% without oxygen inhalation 3–9 days after onset). Serum levels of SCCA and those of IL-4, IL-13, and IFN-γ in some of these patients were measured using a commercially obtained enzyme-linked immunosorbent assay kit (Dinabot Co Ltd, Tokyo, Japan). A SCCA reference range according to a commercial laboratory center is less than 1.5 ng/mL after SCCA-1 and SCCA-2 are totaled.

Informed consent was obtained from the parents of all patients and healthy controls, and this study was approved by our institution's review board. Proper analytical methods, unpaired t test, paired t test, Pearson correlation coefficient, and χ^2 test were applied for each set of data. Data are presented as mean ± SD.

RESULTS

Thirty-five children (24 boys and 11 girls) participated in the study. Seventeen patients had mild persistent asthma, 15

SCCA, ng/mL		CRP, mg/dL	Temperature > 38°C	IL-13, pg/mL		IFN-γ	
Acute phase	Recovery phase			Acute phase	Recovery phase	Acute phase	Recovery phase
2.7	2.2	0.1		10.7		0.11	
3	2.1	1.25	+	9.87		29.4	
5.9	0.9	0.2	+				
3.4	1.6	2.01	+				
5.3	2.6	3.51	+				
1.2	0.3	2.7			7.22		1.56
8.6	1.9	2.04					
1.5	0.9	3.38					
8.8	1.8	1.2	+		33.5		1.56
3.6	1.6	0.49	+	15.2	23.6	112	1.56
2.2	0.7	0.58		29.9	51.1	7.56	10.9
4.2	1.3	1.82	+	18.7		1.56	
1.4	0.8	1.06					
3	2.8	0.34					
5.4	1.6	0.84	+	59.6		28.3	
2.1	1.2	2.38	+				
2.6	0.8	1.64	+				
2.5	1	1.21	+	33.7	28	1.56	1.56
3.5	1.1	2.33	+				
0.7	0.5	1.01					
2	1.7	0.27		11.6	9.56	2	3.12
3.5	1.4	1.07			8.8		1.56
5	1.6	2.17	+				
3.3	1.4	0.62		14.1		1.56	
3.5	0.8	0.18			35.2		1.56
1.9	1.5	0.16		66	52.7	1.56	7.8
5.5	2.1	0.79	+		123		1.56
3.3	2.2	0.14	+				
1.4	1.4	5.37	+				
0.8	1.5	2.78	+	17.7	19.2	4.26	1.56
0.8	1.4	1.84	+				
0.7	0.8	0.06					
2.3	3	7.42			131		1.56
0.7	0.9	0.71					
1.7	2	0.19					

patients had moderate persistent asthma, and 3 patients did not have their conditions categorized because of too short periods since asthma diagnosis. The patients were 4.65 ± 0.57 years of age (age range, 10 months to 14 years), the mean duration of their hospital stay was 7.6 ± 2.1 days, and the mean interval between their acute and recovery investigations was 5.7 ± 2.7 days. Patient disease profiles and characteristics are given in Tables 1 and 2, respectively. Twenty (57%) of the 35 patients had increased C-reactive protein values (>1.0 mg/dL) and 18 (51%) were febrile (temperature, >38.0°C) on admission. All of the patients had upper respiratory tract infections. Before admission, controller medication had been used by 32 (91%) of the 35 patients (Table 1). Regarding glucocorticosteroids, 7 (20%) of the 35 patients were regularly taking inhaled glucocorticosteroids as an controller medicine. Eighteen (51%) of the 35 patients had received an intravenous injection of hydrocortisone at least once in a previous hospital admission for treatment of an asthma attack.

The SCCA levels in control subjects and those in asthma patients at recovery phases are shown in Figure 1. The levels of SCCA in these 2 groups were not significantly different, although the mean value in asthma patients seemed to be higher than that in the controls (P = .12). The patients' SCCA levels at 2 different phases are shown in Figure 2. The acute-phase SCCA level was 3.09 ± 2.03 ng/mL, beyond which the mean serum SCCA level returned to within the reference range (1.47 ± 0.64 ng/mL) during the recovery

Table 2. Patient Characteristics

Characteristic	Finding
M/F	24/11
Age, mean (range), y	4.6 (10–14)
Duration of disease, mean (range), y	2.4 (0–11)
Hospital days, mean ± SD	7.6 ± 2.1
Fever (temperature >38°C), No. (%)	18/35 (51)
CRP >1.0 mg/dL, No. (%)	20/35 (57)
Inhaled corticosteroid use, No. (%)	7/35 (20)
IV corticosteroid use, No. (%)	18/35 (51)
IgE, mean (range), IU/mL	914 (9–10, 535)
RAST result positive for mite, No. (%)	20/26 (77)
RAST result positive for house dust, No. (%)	20/26 (77)
RAST result positive for animal, No. (%)	7/26 (27)

Abbreviations: CRP, C-reactive protein; IV, intravenous; RAST, radioallergosorbent test.

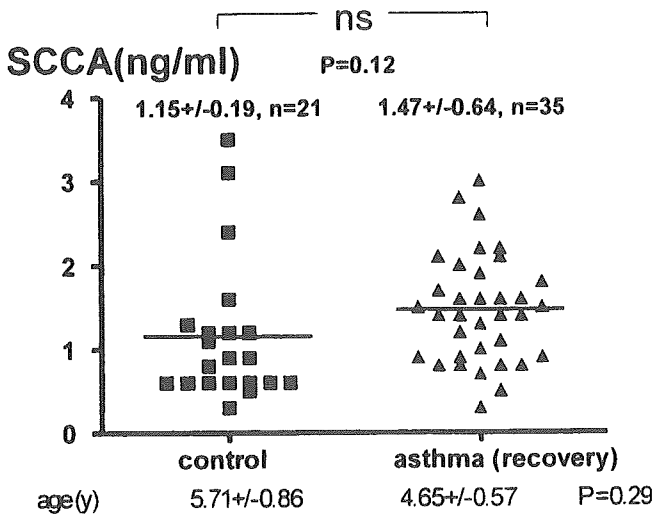

Figure 1. Serum squamous cell carcinoma–related antigen (SCCA) levels in asthma patients and age-matched controls in the recovery phase. No statistically significant difference was found (unpaired *t* test). NS indicates nonsignificant.

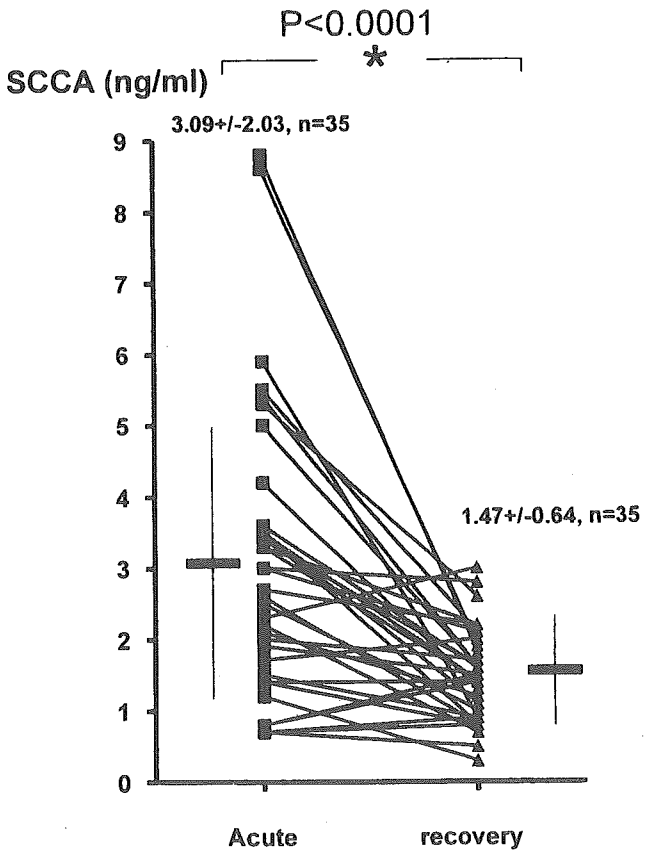

Figure 2. Serum squamous cell carcinoma–related antigen (SCCA) levels in the acute and recovery phases of an asthma attack. A statistically significantly increased mean serum SCCA level was observed in the acute phase compared with the recovery phase (paired *t* test).

phase. Thus, a significantly greater serum SCCA level was observed during the acute phase compared with the recovery phase ($P < .001$). The data were analyzed in 3 different groups of asthma severity (mild persistent, moderate persistent, and undefined groups) and also in 2 different severities of exacerbation (moderate and severe). No differences were found among these subgroups (data not shown).

Serum levels of IgE ($P = .52$ and .66 for the acute and recovery phases, respectively), regular use of inhaled glucocorticosteroids ($P = .68$ and .24 for the acute and recovery phases, respectively), a history of intravenous hydrocortisone injection during an acute attack ($P = .87$ and .41 for the acute and recovery phases, respectively), and the presence of atopic dermatitis ($P = .52$ and .58 for the acute and recovery phases, respectively) were not observed to correlate with increased serum levels of SCCA during both phases of an attack.

Serum levels of IL-13 were measured during the acute phase in 11 patients, during the recovery phase in 12 patients, and in both the acute and recovery phases in 6 patients. Serum levels of IL-13 were not increased during the acute phase of exacerbation compared with those observed in the

recovery phase (Fig 3). We then evaluated the relationship between IL-13 and SCCA levels. The IL-13 levels were observed to correlate with SCCA levels in the recovery phase ($r = .68$, $P = .01$) but not in the acute phase (Fig 4A and B). Levels of IFN-γ were not significantly different in the acute phase when compared with the recovery phase, and no correlation was demonstrated between SCCA and IFN-γ (data not shown). Serum levels of IL-4 were below the limits of detection by enzyme immunoassay.

DISCUSSION

SCCA, which was first identified as a marker of squamous cell carcinoma, is a serine protease inhibitor.[7] A recent study[6] has demonstrated that IL-4 and IL-13 induce marked SCCA expression in cultured human bronchial epithelial cells. This suggests that SCCA might be involved in the pathogenesis of bronchial asthma, since IL-4 and IL-13 are T_H2 cytokines observed in association with chronic eosinophilic inflammation of the airway.[8,9] IL-4 induces class switching of immunoglobulin production to IgE class in B lymphocytes and also activates mast cells.[10] IL-13 induces mucous hypersecretion, subepithelial fibrosis, and eotaxin production within the respiratory epithelium.[11] Thus, IL-4 and IL-13 induce many of the changes seen in allergic diseases, including asthma.

In allergic disorders other than asthma, a potential role for SCCA has been reported. Kawashima et al[5] reported increased SCCA levels in patients with atopic dermatitis. In the present study, however, significantly increased serum SCCA levels were not observed in patients with asthma and atopic dermatitis compared with patients with asthma alone. SCCA may be associated with the state of allergic inflammation of epithelial cells, including airway and skin. Therefore, in asthma exacerbation, the condition of airway epithelial cells may be mainly reflected. Alternatively, there may have been

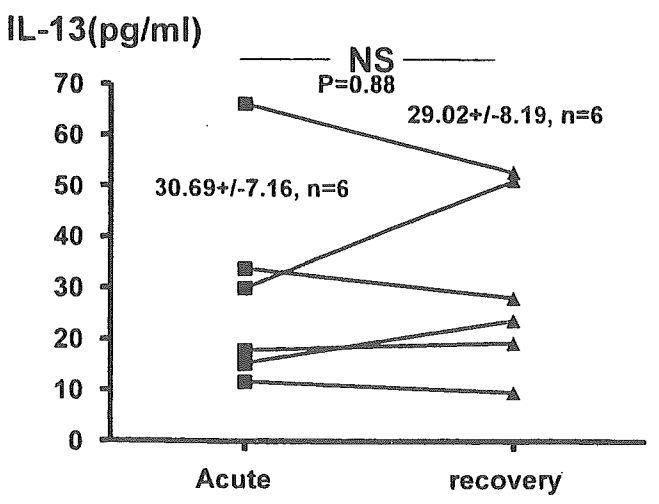

Figure 3. Serum interleukin 13 (IL-13) levels in the acute and recovery phases of an asthma attack. A statistically significant difference in the mean IL-13 level was not observed between the acute and recovery phases (paired *t* test). NS indicates nonsignificant.

differences in the severity of skin lesions between the patients described by Kawashima et al and our patients, who had skin lesions of mild to moderate severity.

In the present study, we observed elevated levels of serum SCCA in the acute phase of an asthma exacerbation, which decreased to within the reference range (<1.5 ng/mL) during the recovery phase, suggesting that SCCA might play a pathophysiologic role in moderate to severe asthma attacks in children. A previous study[6] indicated that SCCA was increased in asthmatic children when compared with a control group. This other study included patients with and without attacks in the same group and compared this group with the control subjects. Therefore, SCCA levels in the asthma group might be higher than those in the control group. The present study confirmed that SCCA was increased only during the acute phase of exacerbation, which might indicate an inflammatory response of airway epithelial cells.

It has been well known that upper respiratory tract infections are closely associated with the exacerbation of asthma in children. In our data, more than 50% of patients (body temperature, >38°C; C-reactive protein, >1.0 mg/mL) had upper respiratory tract infection; however, these inflammatory factors were not significantly correlated with increased SCCA levels (>1.5 ng/mL; for body temperature >38°C, $P = .37$ and .39 for the acute and recovery phases, respectively; for C-reactive protein level of >1.0 mg/mL, $P = .25$ and .24 for the acute and recovery phases, respectively), suggesting that allergic inflammation, but not infectious inflammation, might be associated with an acute reactive production of SCCA in airway epithelial cells.

As indicated previously, IL-4 and IL-13 induce SCCA production in human bronchial epithelial cells in vitro, and IL-13 increases serum SCCA in vivo, suggesting a role for these cytokines in the elevation of SCCA observed during acute exacerbations of asthma.[6] However, our results did not demonstrate a change in IL-13 levels during the acute phase of an asthma exacerbation compared with the recovery phase, suggesting that IL-13 is not associated with the elevation of SCCA observed in the acute phase. On the other hand, serum SCCA levels were correlated with IL-13 levels in the recovery phase, suggesting that IL-13 might contribute to the basal production of SCCA. However, careful evaluation may be required because of limited sample number. Thus, the relationship between IL-13 and SCCA production is still unclear. Other as yet unidentified bioactive substances are also likely involved in the transitory increase in SCCA synthesis seen during the acute phase of an asthma attack. In this study, IL-4 in the samples could not be detected even in the acute phase, suggesting no contribution of IL-4 to SCCA synthesis. Serum IL-4 levels were reported to be very low and close to the sensitivity limit of the assay in asthmatic children.[12]

It is unclear, however, whether SCCA plays a proinflammatory or anti-inflammatory role during an acute asthma attack. As indicated previously, SCCA is a protease inhibitor.[7] Mite Der p 1, a major antigen observed in childhood asthma and rhinitis, is a cysteine protease that acts on several

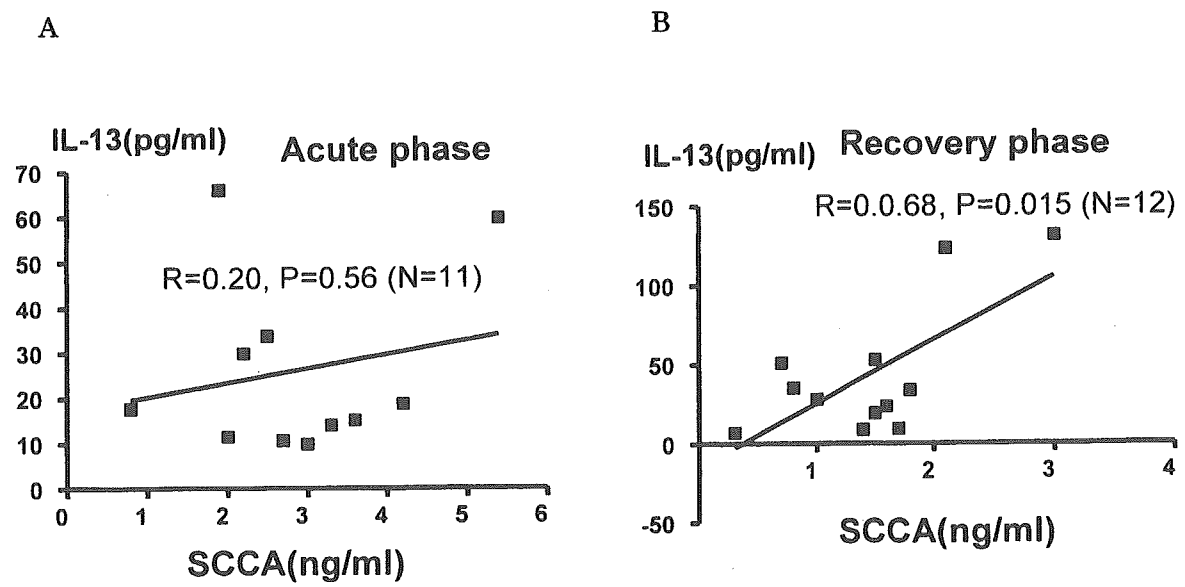

Figure 4. Relationship between serum squamous cell carcinoma–related antigen (SCCA) and interleukin 13 (IL-13) levels during the acute and recovery phases of an asthma attack. A statistically significant correlation was observed between mean IL-13 levels and mean SCCA levels during the recovery phase (A) but not the acute phase (B) (Pearson correlation coefficient).

protein molecules, such as protease-activated receptor 2, CD25, and CD40.[13–15] These protein molecules are converted to bioactive forms by Der p 1. Activated protease-activated receptor 2, for example, increases the production of RANTES, IL-8, and granulocyte-macrophage colony-stimulating factor, which recruit inflammatory cells such as eosinophils and T_H2 lymphocytes to respiratory mucosa, resulting in allergic inflammation.[16,17] Recently, SCCA has been observed to inhibit the protease activity of Der p 1.[18] This context suggests that SCCA may counteract allergic inflammation and function as an anti-inflammatory molecule in vivo. On the other hand, another finding suggests that SCCA may promote the inflammatory process in the airway. SCCA-1 augmented cell growth by attenuating cell apoptosis,[19] indicating that SCCA might promote airway remodeling following allergic airway inflammation. Further studies are needed to clarify the significance and regulation of SCCA production in allergic disease.

ACKNOWLEDGMENTS

This study was partially supported by a grant from the Ministry of Education, Science, Sports, and Culture of Japan (C2 to 14570753).

REFERENCES

1. Kato H, Torigoe T. Radioimmunoassay for tumor antigen of human cervical squamous cell carcinoma. *Cancer.* 1977;40: 1621–1628.
2. Schneider SS, Schick C, Fish KE, et al. A serine proteinase inhibitor locus at 18q21.3 contains a tandem duplication of human squamous cell carcinoma antigen gene. *Proc Natl Acad Sci U S A.* 1995;92:3147–3151.
3. Cataltepe S, Gornstein ER, Schick C, et al. Co-expression of the squamous cell carcinoma antigens 1 and 2 in normal adult human tissues and squamous cell carcinomas. *J Histochem Cytochem.* 2000;48:113–122.
4. Takeshima N, Nakamura K, Takeda O, et al. Individualization of the cutoff value for serum squamous-cell carcinoma antigen using a sensitive enzyme immunoassay. *Tumor Biol.* 1990;11: 167–172.
5. Kawashima H, Nishimata S, Kashiwagi Y, et al. Squamous cell carcinoma-related antigen in children with atopic dermatitis. *Pediatr Int.* 2000;42:448–450.
6. Yuyama N, Davies DE, Akaiwa M, et al. Analysis of novel disease-related genes in bronchial asthma. *Cytokine.* 2002;19: 287–296.
7. Schick C, Kamachi Y, Bartuski AJ, et al. Squamous cell carcinoma antigen 2 is a novel serpin that inhibits the chymotrypsin-like proteinases cathepsin G and mast cell chymase. *J Biol Chem.* 1997;272:1849–1855.
8. Bilenki L, Yang J, Fan Y, Wang S, Yang X. Natural killer T cells contribute to airway eosinophilic inflammation induced by ragweed through enhanced IL-4 and eotaxin production. *Eur J Immunol.* 2004;34:345–354.
9. Vargaftig BB, Singer M. Leukotrienes mediate murine bronchopulmonary hyperreactivity, inflammation, and part of mucosal metaplasia and tissue injury induced by recombinant murine interleukin-13. *Am J Respir Cell Mol Biol.* 2003;28: 410–419.
10. Drazen JM, Arm JP, Austin KF. Sorting out the cytokines of asthma. *J Exp Med.* 1996;183:1–5.
11. Zhu Z, Homer RJ, Wang Z, et al. Pulmonary expression of interleukin-13 causes inflammation, mucus hypersecretion, subepithelial fibrosis, physiologic abnormalities, and eotaxin production. *J Clin Invest.* 1999;103:779–788.
12. Stelmach L, Jerzynska J, Kuna P. Markers of allergic inflam-

mation in peripheral blood of children with asthma after treatment with inhaled triamcinolone acetonide. *Ann Allergy Asthma Immunol.* 2001;87:319–326.
13. Schulz O, Sewell HF, Shakib F. Proteolytic cleavage of CD25, the subunit of the human T cell interleukin 2 receptor, by Der p 1, a major mite allergen with cysteine protease activity. *J Exp Med.* 1998;187:271–275.
14. Ghaemmaghami AM, Gough L, Sewell HF, et al. The proteolytic activity of the major dust mite allergen Der p 1 conditions dendritic cells to produce less interleukin-12: allergen-induced Th2 bias determined at the dendritic cell level. *Clin Exp Allergy.* 2002;32:1468–1475.
15. Asokananthan N, Graham PT, Stewart DJ, et al. House dust mite allergens induce proinflammatory cytokines from respiratory epithelial cells: the cysteine protease allergen, Der p 1, activates protease-activated receptor (PAR)-2 and inactivates PAR-1. *J Immunol.* 2002;169:4572–4578.
16. Stacey MA, Sun G, Vassalli G, Makini M, Bellini A, Mattoli S. The allergen Der p1 induces NF-κB activation through interference with IκBα function in asthmatic bronchial epithelial cells. *Biochem Biophys Res Commun.* 1997;236:522–526.
17. King C, Brennan S, Thompson PJ, Stewart GA. Dust mite proteolytic allergens induce cytokine release from cultured airway epithelium. *J Immunol.* 1998;161:3645–3651.
18. Sakata Y, Arima K, Takai T, et al. The squamous cell carcinoma antigen 2 inhibits the cysteine proteinase activity of a major mite allergen, Der p 1. *J Biol Chem.* 2004;279:5081–5087.
19. Suminami Y, Nagashima S, Murakami A, et al. Suppression of a squamous cell carcinoma(SCC)-related serpin, SCC antigen, inhibits tumor growth with increased intratumor infiltration of natural killer cells. *Cancer Res.* 2001;62:1776–1780.

Requests for reprints should be addressed to:
Yuhei Hamasaki, MD, PhD
Department of Pediatrics
Faculty of Medicine
Saga University
5-1-1 Nabeshima
Saga City 849-8501, Japan
E-mail: hamasaki@post.saga-med.ac.jp